
Deep kernel machines: exact inference with representation learning in infinite Bayesian neural networks

Adam Yang¹

Maxime Robeyns¹

¹University of Bristol, Bristol, UK

Nandi Schoots²

Laurence Aitchison¹

²Kings College London, London, UK

Abstract

Deep neural networks (DNNs) with the flexibility to learn good top-layer representations have eclipsed shallow kernel methods without that flexibility. Here, we take inspiration from DNNs to develop the deep kernel machine. Optimizing the deep kernel machine objective is equivalent to exact Bayesian inference (or noisy gradient descent) in an infinitely wide Bayesian neural network or deep Gaussian process, which has been scaled carefully to retain representation learning. Our work thus has important implications for theoretical understanding of neural networks. In addition, we show that the deep kernel machine objective has more desirable properties and better performance than other choices of objective. Finally, we conjecture that the deep kernel machine objective is unimodal. We give a proof of unimodality for linear kernels, and a number of experiments in the nonlinear case in which all deep kernel machines initializations we tried converged to the same solution.

1 Introduction

Deep neural networks (DNNs Goodfellow et al., 2016) have recently eclipsed kernel methods (Smola & Schölkopf, 1998; Shawe-Taylor & Cristianini, 2004; Hofmann et al., 2008), as DNNs give excellent performance on a wide range of difficult tasks (e.g. Krizhevsky et al., 2012). The key advantage of DNNs is that depth gives the flexibility to learn a good top-layer representation (Aitchison, 2020). In contrast, in a (shallow) kernel method, the kernel itself can be viewed as the top-layer representation (Aitchison, 2020), and this

kernel is highly inflexible — there are usually a few tunable hyperparameters, but nothing that approaches the enormous flexibility of the top-layer representation in a DNN. This raises a critical question: can we take inspiration from *deep* neural networks to develop a *deep* kernel machine, which is able to learn representations? Such a deep kernel machine would represent and optimize a kernel at each layer, rather than weights as in a DNN, or features as in a deep Gaussian process (DGP).

At the same time, there is a completely different line of research on the theory of representation learning in neural networks. Understanding representation learning is difficult because it does not occur in the most theoretically tractable setting of infinite neural networks learned with noisy gradient descent, or equivalently infinite Bayesian neural networks (BNNs; e.g. Aitchison, 2020). Instead, work on representation learning is forced to explicitly consider finite neural networks, which are extremely difficult to reason about. As such, work in this area is forced to use simple settings (shallow/linear) or approximations (e.g. saddle-point or low-order perturbative expansions), which tend to be complex and algebra-heavy (Antognini, 2019; Aitchison, 2020; Li & Sompolinsky, 2020; Yaida, 2020; Naveh et al., 2020; Zavatone-Veth et al., 2021; Zavatone-Veth & Pehlevan, 2021; Roberts et al., 2021; Naveh & Ringel, 2021; Halverson et al., 2021). In contrast, the deep kernel machine embodies a new infinite limit for BNNs where we carefully scale the likelihood as we widen the network such that representation learning is retained. As we still take the infinite limit, we get exact inference (via a Langevin diffusion) even in the full deep, nonlinear setting. Exact inference turns out to be equivalent to optimizing an intuitive objective, formed as a chain of KL-divergences between multivariate Gaussians.

2 Contributions

Here, we introduce the deep kernel machine, which simultaneously gives a practical deep generalisation of kernel methods, and at the same time gives con-

siderable theoretical insight into neural networks, as it corresponds to exact inference in an infinite BNN, which is scaled to ensure that it retains representation learning. In particular,

- We introduce deep kernel machines: a new infinite limit for BNNs which retains representation learning.
- We introduce the deep kernel machine objective, and show that optimizing it is equivalent to *exact* Bayesian inference (Appendix A).
- We introduce a scalable deep kernel machine approach based on Gaussian process inducing points (Appendix C).
- We show that this objective performs better than alternative objectives (Sec 7).
- We show that this objective is unimodal in linear models and give experiments showing convergence to the same solution with different initializations with the deep kernel machine objective, but not with other choices of objective (Sec. 8).

3 Background

3.1 Deep Gaussian processes (DGPs)

A DGP maps from inputs, $\mathbf{X} \in \mathbb{R}^{P \times \nu_0}$, to outputs, $\mathbf{Y} \in \mathbb{R}^{P \times \nu_{L+1}}$, where P is the number of input points, ν_0 is the number of input features, and ν_{L+1} is the number of output features. A DGP has L intermediate layers, indexed $\ell \in \{1, \dots, L\}$, and at each intermediate layer, there are N_ℓ features, $\mathbf{F}_\ell \in \mathbb{R}^{P \times N_\ell}$. The intermediate layer features (i.e. $\mathbf{F}_1, \dots, \mathbf{F}_L$) are sampled from a Gaussian process (GP) with a kernel determined by the features at the previous layer,

$$P(\mathbf{F}_\ell | \mathbf{F}_{\ell-1}) = \prod_{\lambda=1}^{N_\ell} \mathcal{N}(\mathbf{f}_\lambda^\ell; \mathbf{0}, \mathbf{K}_f(\mathbf{F}_{\ell-1})). \quad (1)$$

where \mathbf{f}_λ^ℓ is the activation of the λ th feature for all datapoints, we take $\mathbf{F}_0 = \mathbf{X}$ as the input and \mathbf{K}_f as a function that computes the kernel from the previous layer features. For regression, \mathbf{Y} is Gaussian-process distributed with the usual kernel plus noise,

$$P(\mathbf{Y} | \mathbf{F}_L) = \prod_{\lambda=1}^{\nu_{L+1}} \mathcal{N}(\mathbf{y}_\lambda; \mathbf{0}, \mathbf{K}_f(\mathbf{F}_L) + \sigma^2 \mathbf{I}). \quad (2)$$

For classification, we would use an alternative likelihood e.g. based on a Categorical distribution with softmax probabilities. The feature matrices and outputs can be written as a stack of vectors,

$$\mathbf{F}_\ell = (\mathbf{f}_1^\ell \quad \mathbf{f}_2^\ell \quad \dots \quad \mathbf{f}_{N_\ell}^\ell) \quad (3)$$

$$\mathbf{Y} = (\mathbf{y}_1 \quad \mathbf{y}_2 \quad \dots \quad \mathbf{y}_{\nu_{L+1}}), \quad (4)$$

where each vector gives the value of one output feature for every input example. Results from Aitchison et al.

(2020) establish that the deep Gaussian process probability density can be written entirely in terms of the Gram matrices \mathbf{G}_ℓ

$$\mathbf{G}_\ell = \frac{1}{N_\ell} \mathbf{F}_\ell \mathbf{F}_\ell^T = \frac{1}{N_\ell} \sum_{\lambda=1}^{N_\ell} \mathbf{f}_\lambda^\ell (\mathbf{f}_\lambda^\ell)^T, \quad (5)$$

and does not require full knowledge of the features, \mathbf{F}_ℓ ,

$$\begin{aligned} \log P(\mathbf{F}_\ell | \mathbf{F}_{\ell-1}) + \text{const} & \\ &= -\frac{N_\ell}{2} \log |\mathbf{K}_f(\mathbf{F}_{\ell-1})| - \frac{1}{2} \text{tr}(\mathbf{F}_\ell^T \mathbf{K}_f^{-1}(\mathbf{F}_{\ell-1}) \mathbf{F}_\ell) \\ &= -\frac{N_\ell}{2} \log |\mathbf{K}_f(\mathbf{F}_{\ell-1})| - \frac{N_\ell}{2} \text{tr}(\mathbf{K}_f^{-1}(\mathbf{F}_{\ell-1}) \mathbf{G}_\ell). \end{aligned} \quad (6)$$

However, the log probability still appears to depend on \mathbf{F}_ℓ through the kernel, $\mathbf{K}_f(\mathbf{F}_\ell)$. Remarkably, a large family of kernels, including isotropic kernels that depend only on distance, and non-isotropic kernels such as the arccos kernel (Cho & Saul, 2009) used in the infinite network literature can be written entirely in terms of the Gram matrix (Aitchison et al., 2020). In particular, isotropic kernels depend only on the squared distance, R_{ij}^ℓ ,

$$K_{f;ij}(\mathbf{F}_{\ell-1}) = k(R_{ij}^{\ell-1}), \quad (7)$$

and that squared distance can be recovered from the Gram matrix,

$$\begin{aligned} R_{ij}^\ell &= \frac{1}{N_\ell} \sum_{\lambda=1}^{N_\ell} (F_{i\lambda}^\ell - F_{j\lambda}^\ell)^2 \\ &= \frac{1}{N_\ell} \sum_{\lambda=1}^{N_\ell} ((F_{i\lambda}^\ell)^2 - 2F_{i\lambda}^\ell F_{j\lambda}^\ell + (F_{j\lambda}^\ell)^2) \\ &= G_{ii}^\ell - 2G_{ij}^\ell + G_{jj}^\ell. \end{aligned} \quad (8)$$

Therefore, we can write down $\mathbf{K}(\cdot)$, a function that takes the previous layer's Gram matrix and returns the kernel,

$$\mathbf{K}_f(\mathbf{F}_{\ell-1}) = \mathbf{K}(\mathbf{G}_{\ell-1}) = \mathbf{K}\left(\frac{1}{N_{\ell-1}} \mathbf{F}_{\ell-1} \mathbf{F}_{\ell-1}^T\right). \quad (9)$$

Thus, we can write the probability density for a deep Gaussian process entirely in terms of Gram matrices,

$$\begin{aligned} \log P(\mathbf{F}_\ell | \mathbf{F}_{\ell-1}) &= \log P(\mathbf{F}_\ell | \mathbf{G}_{\ell-1}) \\ &= -\frac{N_\ell}{2} \log |\mathbf{K}(\mathbf{G}_{\ell-1})| - \frac{N_\ell}{2} \text{tr}(\mathbf{K}^{-1}(\mathbf{G}_{\ell-1}) \mathbf{G}_\ell) \\ &\quad + \text{const}. \end{aligned} \quad (10)$$

3.2 (Infinite) Bayesian neural networks are DGPs

Bayesian neural networks are a special case of DGPs (Aitchison, 2020). Consider a neural network of the form,

$$\mathbf{F}_1 = \mathbf{X} \mathbf{W}_0 \quad (11a)$$

$$\mathbf{F}_\ell = \phi(\mathbf{F}_{\ell-1}) \mathbf{W}_{\ell-1} \quad \text{for } \ell \in \{2, \dots, L+1\} \quad (11b)$$

$$W_{\lambda\mu}^\ell \sim \mathcal{N}\left(0, \frac{1}{N_\ell}\right) \quad W_{\lambda\mu}^0 \sim \mathcal{N}\left(0, \frac{1}{\nu_0}\right) \quad (11c)$$

where $\mathbf{W}_0 \in \mathbb{R}^{\nu_0 \times N_1}$, $\mathbf{W}_\ell \in \mathbb{R}^{N_\ell \times N_{\ell+1}}$ and $\mathbf{W}_{L+1} \in \mathbb{R}^{N_L \times \nu_{L+1}}$ are weight matrices with independent Gaussian priors and ϕ is a pointwise nonlinearity. Integrating out the prior over \mathbf{W}_ℓ induces a deep Gaussian process prior over $\mathbf{F}_{\ell+1}$,

$$P(\mathbf{F}_1|\mathbf{X}) = \prod_{\lambda=1}^N \mathcal{N}\left(\mathbf{f}_\lambda^1; \mathbf{0}, \frac{1}{\nu_0} \mathbf{X}\mathbf{X}^T\right) \quad (12a)$$

$$P(\mathbf{F}_\ell|\mathbf{F}_{\ell-1}) = \prod_{\lambda=1}^{N_\ell} \mathcal{N}\left(\mathbf{f}_\lambda^\ell; \mathbf{0}, \mathbf{K}_f(\mathbf{F}_{\ell-1})\right) \quad (12b)$$

$$\mathbf{K}_f(\mathbf{F}_\ell) = \frac{1}{N_\ell} \phi(\mathbf{F}_\ell) \phi^T(\mathbf{F}_\ell). \quad (12c)$$

This is not quite the same DGP as defined in Eq. (1), as we use $\frac{1}{\nu_0} \mathbf{X}\mathbf{X}^T$ rather than $\mathbf{K}_f(\mathbf{F}_{\ell-1})$ as the first-layer kernel; but it is still a DGP. In addition, Eq. (12c) might seem like a strange kernel, as it does not take on one of the standard forms, such as a squared exponential or Matern. But it is a perfectly valid kernel, as it is the product of (transformed) feature vectors, $\phi(\mathbf{F}_\ell)$, and thus Bayesian neural networks are a special case of DGPs.

The issue for deep kernel machines is that this kernel depends explicitly on the features, and cannot be written solely as a function of the Gram matrix. However, this feature-dependence disappears as we take the infinite limit (in particular, $N_\ell \rightarrow \infty$),

$$\begin{aligned} \lim_{N_\ell \rightarrow \infty} K_{f;ij}(\mathbf{F}_\ell) &= \lim_{N_\ell \rightarrow \infty} \frac{1}{N_\ell} \sum_{\lambda=1}^{N_\ell} \phi(F_{i\lambda}^\ell) \phi(F_{j\lambda}^\ell) \\ &= \mathbb{E} [\phi(F_{i\lambda}^\ell) \phi(F_{j\lambda}^\ell)] \\ &= K_{ij}(\mathbf{G}_\ell) \end{aligned} \quad (13)$$

where the second line comes from applying the law of large numbers, as this is an average of infinitely many IID terms. The actual functional form for the kernels on the third line comes from Cho & Saul (2009), who gave analytic form for nonlinearities of the form $\phi(x) = x^n \Theta(x)$ as a function of the Gram matrix (where $\Theta(x)$ is the Heaviside step function, which is one when $x > 0$, and zero otherwise), and these results are commonly applied in the infinite neural network literature. Note that this approach works for the prior, but there are subtleties when applying it to the posterior (Appendix B).

4 Deriving the deep kernel machine objective

We consider an infinitely wide DGP obtained by setting

$$N_\ell = N \nu_\ell \quad \text{for} \quad \ell \in \{1, \dots, L+1\} \quad (14)$$

with ν_ℓ finite and $N \rightarrow \infty$. As shown by e.g. Aitchison (2020), an infinitely wide BNN/DGP does not exhibit any representation learning, as the learned Gram matrices and kernels converge to their values under the prior.

Our key insight was that we can retain representation learning by replicating the data N times,

$$\tilde{\mathbf{Y}} = (\mathbf{Y} \quad \dots \quad \mathbf{Y}) \quad (15)$$

where $\mathbf{Y} \in \mathbb{R}^{P \times \nu_{L+1}}$, so $\tilde{\mathbf{Y}} \in \mathbb{R}^{P \times N_{L+1}}$, and by using a likelihood which assumes each copy of \mathbf{Y} is independent,

$$\log P(\tilde{\mathbf{Y}}|\mathbf{G}_L) = N \log P(\mathbf{Y}|\mathbf{G}_L). \quad (16)$$

Finally, note that we take *one* limit, $N \rightarrow \infty$, which simultaneously takes all layer widths, N_1, \dots, N_L , and the data width, N_{L+1} , to infinity. Thus, we do not encounter issues arising from taking limits in sequence discussed in Matthews et al. (2018).

The most direct way to derive the deep kernel machine objective uses variational inference. In particular, consider a variational approximate posterior over features,

$$Q(\mathbf{F}_\ell) = \prod_{\lambda=1}^{N_\ell} \mathcal{N}(\mathbf{f}_\lambda^\ell; \mathbf{0}, \boldsymbol{\Sigma}_\ell) \quad (17)$$

Note that \mathbf{G}_ℓ (Eq. 5) is not necessarily equal to the covariance of the approximate posterior, $\boldsymbol{\Sigma}_\ell$, in the finite setting, but they do become equal in the infinite limit. In particular, note that the Gram matrix can be written as the average of N_ℓ IID terms, $\mathbf{f}_\lambda^\ell (\mathbf{f}_\lambda^\ell)^T$ (Eq. 5). In the infinite limit the law of large numbers tells us that the average becomes equal to its expectation,

$$\begin{aligned} \lim_{N_\ell \rightarrow \infty} \mathbf{G}_\ell &= \lim_{N_\ell \rightarrow \infty} \frac{1}{N_\ell} \sum_{\lambda=1}^{N_\ell} \mathbf{f}_\lambda^\ell (\mathbf{f}_\lambda^\ell)^T \\ &= \mathbb{E} [\mathbf{f}_\lambda^\ell (\mathbf{f}_\lambda^\ell)^T] = \boldsymbol{\Sigma}_\ell. \end{aligned} \quad (18)$$

Thus, in the infinite limit, the approximate posterior can be parameterised by the Gram matrices themselves,

$$Q(\mathbf{F}_\ell) = \prod_{\lambda=1}^{N_\ell} \mathcal{N}(\mathbf{f}_\lambda^\ell; \mathbf{0}, \mathbf{G}_\ell) \quad (19)$$

And the variational inference objective, the ELBO, can be written as a function of the approximate posterior parameters, $\mathbf{G}_1, \dots, \mathbf{G}_L$,

$$\begin{aligned} \text{ELBO}(\mathbf{G}_1, \dots, \mathbf{G}_L) &= \mathbb{E}_{Q(\mathbf{F}_1, \dots, \mathbf{F}_L)} [\log P(\tilde{\mathbf{Y}}|\mathbf{G}_L) \\ &+ \sum_{\ell=1}^L \log P(\mathbf{F}_\ell|\mathbf{F}_{\ell-1})] + H[Q(\mathbf{F}_1, \dots, \mathbf{F}_L)] \end{aligned} \quad (20)$$

where $H[Q(\mathbf{F}_1, \dots, \mathbf{F}_L)]$ is the entropy of the approximate posterior. Remember that $\log P(\mathbf{F}_\ell|\mathbf{F}_{\ell-1})$ depends only on the Gram matrix (Eq. 10), and in the infinite limit the Gram matrix is deterministic. Thus, evaluating the expectation and the entropy, we obtain,

$$\begin{aligned} \text{ELBO}(\mathbf{G}_1, \dots, \mathbf{G}_L) &= \log P(\tilde{\mathbf{Y}}|\mathbf{G}_L) \\ &+ \sum_{\ell=1}^L (\log P(\mathbf{F}_\ell|\mathbf{F}_{\ell-1}) + \frac{N_\ell}{2} \log |\mathbf{G}_\ell|). \end{aligned} \quad (21)$$

The log-determinant terms, $\log |\mathbf{G}_\ell|$, arise from the entropy and can be understood as representing the volume

in feature-space corresponding to the Gram matrix (see Sec. 8 and in particular Eq. 35). Substituting Eq. 10,

$$\begin{aligned} \text{ELBO}(\mathbf{G}_1, \dots, \mathbf{G}_L) &= \log P(\tilde{\mathbf{Y}}|\mathbf{G}_L) \\ &+ \sum_{\ell=1}^L \frac{\nu_\ell}{2} (\log |\mathbf{K}^{-1}(\mathbf{G}_{\ell-1})\mathbf{G}_\ell| \\ &- \text{tr}(\mathbf{K}^{-1}(\mathbf{G}_{\ell-1})\mathbf{G}_\ell)). \end{aligned} \quad (22)$$

The ELBO will become infinite as $N \rightarrow \infty$. To ensure that the deep kernel machine objective remains finite we define it as,

$$\mathcal{L}(\mathbf{G}_1, \dots, \mathbf{G}_L) = \frac{1}{N} \text{ELBO}(\mathbf{G}_1, \dots, \mathbf{G}_L). \quad (23)$$

Writing this out concretely,

$$\begin{aligned} \mathcal{L}(\mathbf{G}_1, \dots, \mathbf{G}_L) &= \log P(\mathbf{Y}|\mathbf{G}_L) \\ &+ \sum_{\ell=1}^L \frac{\nu_\ell}{2} (\log |\mathbf{K}^{-1}(\mathbf{G}_{\ell-1})\mathbf{G}_\ell| \\ &- \text{tr}(\mathbf{K}^{-1}(\mathbf{G}_{\ell-1})\mathbf{G}_\ell)), \end{aligned} \quad (24)$$

where, remember, ν_ℓ are fixed and finite and \mathbf{Y} is the original data, before copying. Remarkably, exactly the same objective can be obtained by considering a very different inference approach: Langevin sampling. In particular, in the infinite width limit, Langevin dynamics become deterministic, and equivalent to (preconditioned) gradient descent on this objective (Appendix A). Thus, the derivation of the objective is not restricted to e.g. a particular choice of variational approximate posteriors — this is just the most straightforward derivation, but others (such as the Langevin sampling derivation in Appendix A) exist.

5 Theoretical understanding of BNNs

The power of the deep kernel machine as a theoretical technique for understanding representation learning in neural networks is evident if we rewrite the objective as a sum of KL-divergences of multivariate Gaussian distributions with covariance \mathbf{G}_ℓ and $\mathbf{K}(\mathbf{G}_{\ell-1})$,

$$\begin{aligned} \mathcal{L}(\mathbf{G}_1, \dots, \mathbf{G}_L) &= \log P(\mathbf{Y}|\mathbf{G}_L) + \text{const} \quad (25) \\ &- \sum_{\ell=1}^L \nu_\ell D_{\text{KL}}(\mathcal{N}(\mathbf{0}, \mathbf{G}_\ell) \parallel \mathcal{N}(\mathbf{0}, \mathbf{K}(\mathbf{G}_{\ell-1}))) \end{aligned}$$

Thus, the “prior” terms formulated here as KL-divergences act as a strong regulariser, ensuring that \mathbf{G}_ℓ is close to $\mathbf{K}(\mathbf{G}_{\ell-1})$. At the same time, the likelihood, $\log P(\mathbf{Y}|\mathbf{G}_L)$, encourages us to find a representation giving good performance on the training data. Of course we could use any form for $P(\mathbf{Y}|\mathbf{G}_L)$, including both classification and regression. To understand how the likelihood interacts with the prior terms, it is easiest to consider regression,

$$P(\mathbf{Y}|\mathbf{G}_L) = \prod_{\lambda=1}^{\nu_{L+1}} \mathcal{N}(y_\lambda; \mathbf{0}, \mathbf{K}(\mathbf{G}_L) + \sigma^2 \mathbf{I}). \quad (26)$$

This log-likelihood can be written as a KL-divergence

$$\begin{aligned} \log P(\mathbf{Y}|\mathbf{G}_L) &= \text{const} \quad (27) \\ &- \nu_{L+1} D_{\text{KL}}(\mathcal{N}(\mathbf{0}, \mathbf{G}_{L+1}) \parallel \mathcal{N}(\mathbf{0}, \mathbf{K}(\mathbf{G}_L) + \sigma^2 \mathbf{I})) \end{aligned}$$

Thus, the likelihood term encourages $\mathbf{K}(\mathbf{G}_L) + \sigma^2 \mathbf{I}$ to be as possible to the covariance of the data, $\mathbf{G}_{L+1} = \frac{1}{\nu_{L+1}} \mathbf{Y}\mathbf{Y}^T$. Combining this likelihood with Eq. (25), we would expect deep kernel machine to find a sequence of \mathbf{G}_ℓ that smoothly “interpolate” between the input kernel, \mathbf{G}_0 and the output kernel, \mathbf{G}_{L+1} . Indeed, this notion of smooth interpolation can be formulated explicitly in the case of a linear kernel (Sec. 8.1).

6 An alternative MAP objective

A more obvious objective could be based on MAP,

$$\begin{aligned} \mathcal{L}_{\text{MAP}}(\mathbf{G}_1, \dots, \mathbf{G}_L) &= \frac{1}{N} (\log P(\tilde{\mathbf{Y}}|\mathbf{G}_L) \\ &+ \sum_{\ell=1}^L \log P(\mathbf{F}_\ell|\mathbf{F}_{\ell-1})) \end{aligned} \quad (28)$$

As before, we have divided by N to ensure that the objective remains finite as $N \rightarrow \infty$. Substituting Eq. (10), we get a form very similar to Eq. (24), but lacking $\log |\mathbf{G}_\ell|$,

$$\begin{aligned} \mathcal{L}_{\text{MAP}}(\mathbf{G}_1, \dots, \mathbf{G}_L) &= \log P(\mathbf{Y}|\mathbf{G}_L) \\ &+ \sum_{\ell=1}^L \frac{\nu_\ell}{2} (\log |\mathbf{K}_\ell^{-1}(\mathbf{G}_{\ell-1})| \\ &- \text{tr}(\mathbf{K}_\ell^{-1}(\mathbf{G}_{\ell-1})\mathbf{G}_\ell)). \end{aligned} \quad (29)$$

Before explicitly testing performance, it is worth noting that MAP objectives have theoretical deficiencies. In particular, we probably want the deep kernel machine objective to behave sensibly when little or no data is available. In particular, we would like the Gram matrix to converge to its value under the prior. Taking a one intermediate layer deep kernel machine with no data for simplicity, we would like,

$$\mathbf{K}(\mathbf{G}_0) = \arg \max_{\mathbf{G}_1} \mathcal{L}(\mathbf{G}_1). \quad (30)$$

In this setting, the deep kernel machine objective is,

$$\mathcal{L}(\mathbf{G}_1) = -\nu_1 D_{\text{KL}}(\mathcal{N}(\mathbf{0}, \mathbf{G}_1) \parallel \mathcal{N}(\mathbf{0}, \mathbf{K}(\mathbf{G}_0))) \quad (31)$$

which clearly is maximized at $\mathbf{G}_1 = \mathbf{K}(\mathbf{G}_0)$. However, this is not true for the MAP objective,

$$\mathbf{0} = \arg \max_{\mathbf{G}_\ell} [\log P(\mathbf{F}_\ell|\mathbf{F}_{\ell-1})]. \quad (32)$$

so the MAP objective will give pathological solutions when little or no data is available.

7 Performance of different objectives

Here, we compare the performance of the deep kernel machine objective (Eq. 24) and the MAP objective (Eq. 29). In addition, we considered a baseline, which was a standard, shallow kernel method mirroring the structure of the deep kernel machine but where the only flexibility comes from the hyperparameters. Formally, this model can be obtained by setting,

$$\mathbf{G}_\ell = \mathbf{K}(\mathbf{G}_{\ell-1}), \quad (33)$$

and is denoted ‘‘Kernel Hyper’’ in Table 1.

We applied these methods to UCI datasets Gal & Ghahramani (2016). We used a two hidden layer architecture, with a kernel inspired by the skip-connections used in Salimbeni & Deisenroth (2017). In particular, we used,

$$\mathbf{K}(\mathbf{G}_\ell) = w_1^\ell \mathbf{G}_\ell + w_2^\ell \mathbf{K}_{\text{sqexp}}(\mathbf{G}_\ell) \quad (34)$$

where w_1^ℓ , w_2^ℓ and σ are hyperparameters, and $\mathbf{K}_{\text{sqexp}}(\mathbf{G}_\ell)$ is a standard squared-exponential kernel.

Inspired by GPs, we designed a scalable inducing point inference method, (Appendix C), and used 300 inducing points fixed to a random subset of the training data and not further optimised during training.

We ran the training procedure using the Adam optimizer with a learning rate of 0.001 and full-batch gradient steps. We used 5000 iterations for smaller datasets and 1000 iterations for larger datasets (kin8nm, naval and protein).

We found that the deep kernel machine objective gave better performance than MAP, or the hyperparameter optimization baseline (Tab. 1). While these numbers look reasonable compared to those in the deep GP literature (e.g. Salimbeni & Deisenroth, 2017), they are not directly comparable, as deep GPs are fully Bayesian, while deep kernel machines are not (as they replicate the data infinitely many times). Thus, deep kernel machines cannot offer the same protection against overfitting given by a true Bayesian method.

8 Unimodality

One of the main practical motivations for moving from features or weights to Gram matrices is that we have strong reason to believe objectives and posteriors are much better behaved in the space of Gram matrices (Aitchison et al., 2020). In particular, remember that the log-probability, $P(\mathbf{F}_\ell | \mathbf{F}_{\ell-1})$ (Eq. 10) depended only on the Gram matrices, meaning that for one optimal Gram matrix, there is an infinite family of optimal features, parameterised by a unitary transformation,

Table 1: RMSE for inducing point methods. (Equal best methods are displayed in bold. Error bars give two stderrs for a paired tests, which uses differences in performance between that method and best method, (so there are no meaningful error bars on the best performing method itself). The method using the MAP objective did not run to completion on the boston dataset, due to numerical instability.

dataset	Kernel Hyper	MAP	\mathcal{L}
boston	4.41 ± 0.31	—	4.35 ± 0.51
concrete	5.38 ± 0.098	5.60 ± 0.15	5.10
energy	0.83 ± 0.076	0.73 ± 0.049	0.47
kin8nm	$(7.3 \pm 0.06) \cdot 10^{-2}$	$(7.4 \pm 0.05) \cdot 10^{-2}$	$6.6 \cdot 10^{-2}$
naval	$(6.4 \pm 0.6) \cdot 10^{-4}$	$(5.4 \pm 0.5) \cdot 10^{-4}$	$4.6 \cdot 10^{-4}$
yacht	0.94 ± 0.058	1.14 ± 0.077	0.58
power	3.81 ± 0.091	3.73 ± 0.14	3.58
protein	4.21 ± 0.029	4.30 ± 0.033	4.10
wine	0.68 ± 0.0084	0.66 ± 0.0067	0.64

$\mathbf{U} \in \mathbb{R}^{N_\ell \times N_\ell}$ satisfying $\mathbf{U}\mathbf{U}^T = \mathbf{I}$. To confirm, consider computing the Gram matrix, \mathbf{G}'_ℓ for a unitary transformation of the features, $\mathbf{F}'_\ell = \mathbf{F}_\ell \mathbf{U}$,

$$\mathbf{G}'_\ell = \frac{1}{N_\ell} \mathbf{F}'_\ell \mathbf{F}'_\ell{}^T = \frac{1}{N_\ell} \mathbf{F}_\ell \mathbf{U} \mathbf{U}^T \mathbf{F}_\ell^T = \frac{1}{N_\ell} \mathbf{F}_\ell \mathbf{F}_\ell^T = \mathbf{G}_\ell \quad (35)$$

Thus, the objective landscape is far more complex in the feature domain than when working with the Gram matrix. While this argument establishes that the objective landscape for Gram matrices is simpler than that for features, it leaves open the question of whether the objective landscape for Gram matrices is actually unimodal. As such, we begin by giving a proof of unimodality in the linear case. As we do not yet have a proof of unimodality in the nonlinear case, we instead did a number of experiments, by using many different random initializations of a deep kernel machine and optimizing using gradient descent. For all initializations we considered, the deep kernel machine objective converged to the same solution, which was not true for the MAP objective.

8.1 Unimodality with a linear kernel

Here, we show that the deep kernel machine objective is unimodal for a linear kernel. A linear kernel simply returns the input Gram matrix,

$$\mathbf{K}(\mathbf{G}) = \mathbf{G}. \quad (36)$$

It is called a linear kernel, because it arises in the neural network setting (Eq. 11) by choosing the nonlinearity, ϕ to be the identity, in which case, $\mathbf{F}_\ell = \mathbf{F}_{\ell-1} \mathbf{W}_{\ell-1}$.

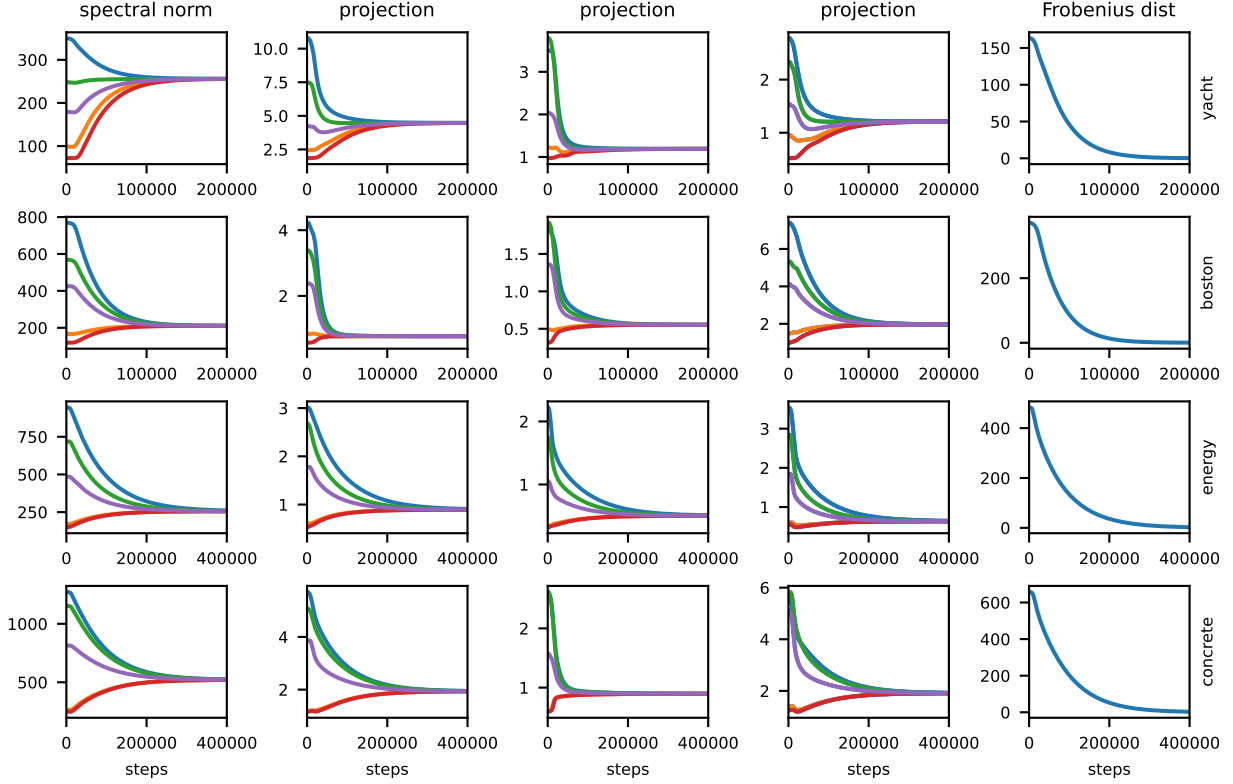


Figure 1: One-layer deep kernel machine with a squared-exponential kernel trained on yacht, boston, energy and concrete.

For a linear kernel the objective becomes,

$$\mathcal{L}(\mathbf{G}_1, \dots, \mathbf{G}_L) = \sum_{\ell=1}^{L+1} \frac{\nu_\ell}{2} (\log |\mathbf{G}_{\ell-1}^{-1} \mathbf{G}_\ell| - \text{Tr}(\mathbf{G}_{\ell-1}^{-1} \mathbf{G}_\ell)) \quad (37)$$

where we have assumed there is no output noise, $\sigma^2 = 0$. Taking all ν_ℓ to be equal, $\nu = \nu_\ell$ (see Appendix D for the general case),

$$\mathcal{L}(\mathbf{G}_1, \dots, \mathbf{G}_L) = \log |\mathbf{G}_0^{-1} \mathbf{G}_{L+1}| - \frac{\nu}{2} \sum_{\ell=1}^{L+1} \text{Tr}(\mathbf{G}_{\ell-1}^{-1} \mathbf{G}_\ell). \quad (38)$$

To find the mode, we set the gradient wrt \mathbf{G}_ℓ to zero,

$$\mathbf{0} = \frac{\partial \mathcal{L}}{\partial \mathbf{G}_\ell} = \frac{\nu}{2} (\mathbf{G}_{\ell-1}^{-1} - \mathbf{G}_\ell^{-1} \mathbf{G}_{\ell+1} \mathbf{G}_\ell^{-1}) \quad (39)$$

Thus, at the mode, the recursive relationship must hold,

$$\mathbf{T} = \mathbf{G}_{\ell-1}^{-1} \mathbf{G}_\ell = \mathbf{G}_\ell^{-1} \mathbf{G}_{\ell+1}. \quad (40)$$

Thus, optimal Gram matrices are given by,

$$\mathbf{G}_\ell = \mathbf{G}_0 \mathbf{T}^\ell, \quad (41)$$

and we can solve for \mathbf{T} by noting,

$$\mathbf{G}_0^{-1} \mathbf{G}_{L+1} = \mathbf{T}^{L+1}. \quad (42)$$

Importantly, \mathbf{T} is the product of two positive definite matrices, $\mathbf{T} = \mathbf{G}_{\ell-1}^{-1} \mathbf{G}_\ell$, so \mathbf{T} must have positive, real eigenvalues (but \mathbf{T} does not have to be symmetric Horn & Johnson, 2012). There is only one solution to Eq. (42) with positive real eigenvalues (Horn et al., 1994). Intuitively, this can be seen using the eigendecomposition, $\mathbf{G}_0^{-1} \mathbf{G}_{L+1} = \mathbf{V}^{-1} \mathbf{D} \mathbf{V}$, where \mathbf{D} is diagonal,

$$\mathbf{T} = (\mathbf{V}^{-1} \mathbf{D} \mathbf{V})^{1/(L+1)} = \mathbf{V}^{-1} \mathbf{D}^{1/(L+1)} \mathbf{V}. \quad (43)$$

Thus, finding \mathbf{T} reduces to finding the $(L+1)$ th root of each positive real number on the diagonal of \mathbf{D} . While there are $(L+1)$ complex roots, there is only one positive real root, and so \mathbf{T} and hence $\mathbf{G}_1, \dots, \mathbf{G}_L$ are uniquely specified by setting the gradient of the objective to zero. This contrasts with a deep linear neural network, which has infinitely many optimal settings for the weights lying on a complex manifold.

Note that for the objective to be well-defined, we need $\mathbf{K}(\mathbf{G})$ to be full-rank. With standard kernels (such as the squared exponential) this is always the case, even if the input Gram matrix is singular. However, a linear kernel will have a singular output if given a singular input, and with enough data points, $\mathbf{G}_0 = \frac{1}{\nu_0} \mathbf{X} \mathbf{X}^T$ is always singular. To fix this, we redefine \mathbf{G}_0 to be the result of a positive definite kernel applied to $\frac{1}{\nu_0} \mathbf{X} \mathbf{X}^T$,

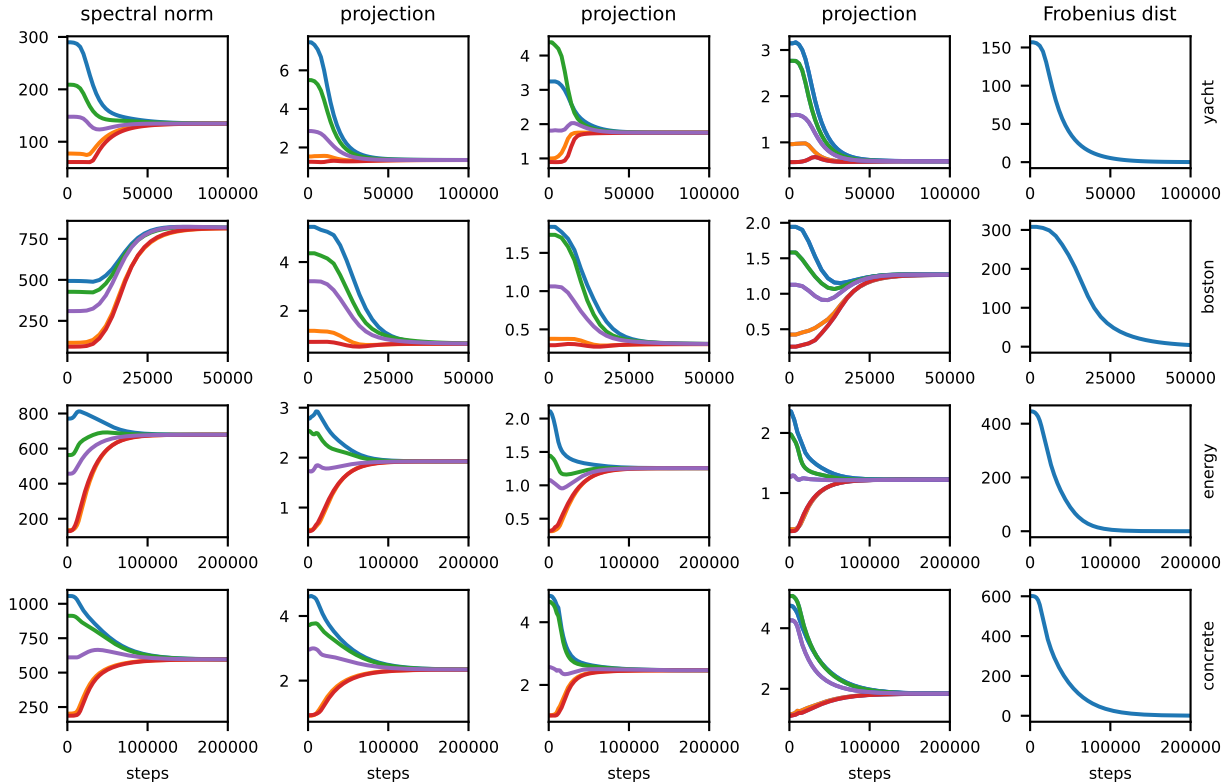


Figure 2: One-layer deep kernel machine with ReLU kernel trained on yacht, boston, energy and concrete.

which results in \mathbf{G}_0 being full-rank, as long as the input points are distinct.

8.2 Unimodality with nonlinear kernels

Here, we confirm empirically that gradient descent on the deep kernel machine objective with a nonlinear kernel does indeed converge to the same solution, no matter the initial condition. We parameterise Gram matrices $\mathbf{G}_\ell = \frac{1}{P} \mathbf{V}_\ell \mathbf{V}_\ell^T$ with $\mathbf{V}_\ell \in \mathbb{R}^{P \times P}$ being trainable parameters.

To make initializations with different seeds sufficiently separated while ensuring stability we initialize \mathbf{G}_ℓ from a broad distribution that depends on $\mathbf{K}(\mathbf{G}_{\ell-1})$. Specifically, we take the Cholesky decomposition of the kernel at the previous layer, $\mathbf{K}(\mathbf{G}_{\ell-1}) = \mathbf{L}_{\ell-1} \mathbf{L}_{\ell-1}^T$ and then set $\mathbf{V}_\ell = \mathbf{L}_{\ell-1} \mathbf{\Xi}_\ell \mathbf{D}_\ell^{1/2}$ where each entry of $\mathbf{\Xi}_\ell \in \mathbb{R}^{P \times P}$ is independently sampled from a standard Gaussian, and \mathbf{D}_ℓ is a diagonal scaling matrix with each entry sampled from an inverse-Gamma distribution to scale different initializations sufficiently distinct (see Appendix F for more details).

To evaluate convergence, we plot the trajectory across training of the spectral norm of the Gram matrix and three random projections $\mathbf{x}^T \mathbf{G}_\ell \mathbf{x}$, where each $\mathbf{x} \in \mathbb{R}^{P \times 1}$

is sampled from uniform Gaussian and stays fixed for different initializations. In addition, we plot the average Frobenius distance for each pair of initializations,

$$D_F := \frac{1}{\frac{1}{2}n(n-1)} \sum_{i=1}^{n-1} \sum_{j=i+1}^n \|\mathbf{G}_\ell^{(i)} - \mathbf{G}_\ell^{(j)}\|_F, \quad (44)$$

where $\mathbf{G}_\ell^{(i)}$ denotes the i th initialization of \mathbf{G}_ℓ , and $\frac{1}{2}n(n-1)$ is the total number of pairs given n initializations in total. As the Gram matrices converge, the Frobenius distance should also tend to zero.

We set $\nu_\ell = 20$, and use the Adam optimizer (Kingma & Ba, 2014) with learning rate 0.001 to optimize parameters \mathbf{V}_ℓ described above. We fixed all hyperparameters to ensure that any multimodality could emerge only from the underlying deep kernel machine. As we did not use inducing points, we were forced to consider only the smaller UCI datasets (yacht, boston, energy and concrete). For the deep kernel machine objective, all Gram matrices converge rapidly to the same solution, as measured in terms of spectral norms, projections and the Frobenius distance (Fig. 1, 2, 4–11). Critically, we did find multiple modes for the MAP objective on yacht (Fig 3), indicating that experiments are indeed powerful enough to find multiple modes (though of course they cannot be guaranteed to find them). Fi-

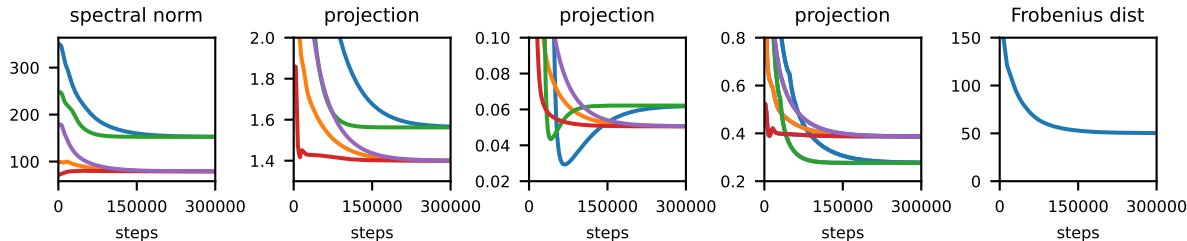


Figure 3: One-layer deep kernel machine with squared-exponential kernel trained on yacht using the MAP objective, where the same initialization scheme finds two solutions.

nally, note that the Gram matrices took a surprisingly long time to converge: this was largely due to the high degree of diversity in the initializations; convergence was much faster if we initialised deterministically from the prior as in Sec. 6.

9 Related work

The neural tangent kernel (NTK) literature attempts to analyse the dynamics of gradient descent in neural networks, by considering the infinite limit. This is very different from our setting, which considers optimal Bayesian neural networks, or equivalent neural networks trained with noisy gradient descent. In the usual NTK setting, the particular infinite limit taken prohibits representation learning, and thus fails to mirror the behaviour of real neural networks. Yang & Hu (2020) solved this issue, describing a limit which does exhibit representation learning, by careful choice of the right initialization and parameterisation. This is a valuable line of work that resolves longstanding technical issues with the NTK. But it does not address the problem of how to give a deep generalisation of kernel methods, and nor does it set out to: Yang & Hu (2020) themselves state that their work is very different to deep kernel methods (their Related Work Section). Moreover, the practicality of their framework remains to be established: their experiments were performed on linear one-hidden layer networks, which admit considerable simplification under their approach (Yang & Hu, 2020, their Sec. 9.2: Models and Alg. 2 and 3). In contrast, one of our goals was to develop the foundations for practical deep kernel methods, so we designed objectives and dynamics specifically for the infinite limit which were dramatically different from gradient descent (see Sec. A). In contrast to Yang & Hu (2020), our approach enables straightforward practical use in deep nonlinear networks, can be implemented directly using modern autodiff, and can be combined with a variety of methods from the kernel literature.

There is a body of work using methodology from physics to understand representation learning in neural net-

works (Antognini, 2019; Aitchison, 2020; Li & Sompolinsky, 2020; Yaida, 2020; Naveh et al., 2020; Zavatone-Veth et al., 2021; Zavatone-Veth & Pehlevan, 2021; Roberts et al., 2021; Naveh & Ringel, 2021; Halverson et al., 2021). However, this work explicitly considers finite networks, and therefore is forced to use inexact low-order perturbative expansions (and in addition, tends to be complex, algebra-heavy, and unintuitive). In contrast, we introduce a new infinite limit for Bayesian neural networks with all the analytic tractability of standard infinite limits, but retaining representation learning by scaling the likelihood term as we widen the network. This approach gives a simple, intuitive, exact understanding of representation learning in infinite neural networks as aligning \mathbf{G}_ℓ with $\mathbf{K}(\mathbf{G}_{\ell-1})$ in the lower layers, and aligning the top layer representation, $\mathbf{K}(\mathbf{G}_L)$, with $\mathbf{G}_{L+1} = \frac{1}{Y_{L+1}} \mathbf{Y}\mathbf{Y}^T$. The degree of alignment is measured as the KL-divergence between multivariate Gaussians with these covariances (Eq. 25). As such, our work also has implications for the study of “feature alignment”, which understands this process of aligning the top-layer representation as a form of implicit regularisation (Aitchison, 2020; Baratin et al., 2021; Lou et al., 2021).

An alternative line of work on deep kernel *processes* (rather than our *machines*) (Aitchison et al., 2020; Ober & Aitchison, 2021) uses fully Bayesian deep nonlinear function approximators that optimize a variational approximate posterior over Gram matrices. This is problematic, as appropriate approximate posteriors over matrices remain poorly understood, and the sampling required by variational inference adds considerable variance to the gradient estimator. In contrast, the deep kernel machine setting is much simpler, as we deterministically optimize the Gram matrices. The deep kernel machine thus offers theoretical insights through its extremely simple, interpretable loss function (Eq. 25) derived through exact inference, and allows an analysis of unimodality that are unavailable to deep kernel processes.

Another related line of work uses kernels to give a closed-form expression for the weights of a neural net-

work, based on a greedy, layerwise objective (Wu et al., 2022). This work differs in that it uses the HSIC objective, and therefore does not have a link to DGPs or Bayesian neural networks, and in that it uses a greedy-layerwise objective, rather than end-to-end gradient descent.

Finally, our work has implications for understanding convergence and loss-landscapes in NNs and DGPs. In particular, we have conjectured that the deep kernel machine objective is unimodal, which would suggest that multimodality in DGPs arises solely from the unitary symmetries Eq. (35), and that multimodality in NNs arises from permutation symmetries, where the exact same input-output function can be achieved by swapping the identities of the intermediate layer weights (MacKay, 1992; Chen et al., 1993). This hypothesis was recently conjectured for finite neural networks (Entezari et al., 2021) as a potential explanation of mode connectivity (Garipov et al., 2018).

10 Conclusion

In this work, we introduced the deep kernel machine objective, and showed that it corresponds to exact inference in an infinite BNN (specifically, gradient descent corresponds to a Langevin diffusion). We showed theoretically and experimentally that the deep kernel machine objective gives better performance than other approaches such as a MAP objective. Finally, we analysed the unimodality of the deep kernel machines objective. We proved unimodality in the case of a linear kernel. As we were not able to provide a proof for the nonlinear case, we instead gave experimental results: all initializations we considered converged to the same solution under the deep kernel machine objective.

References

- Aitchison, L. Why bigger is not always better: on finite and infinite neural networks. In *International Conference on Machine Learning*, pp. 156–164. PMLR, 2020.
- Aitchison, L., Yang, A. X., and Ober, S. W. Deep kernel processes. *arXiv preprint arXiv:2010.01590*, 2020.
- Antognini, J. M. Finite size corrections for neural network gaussian processes. *arXiv preprint arXiv:1908.10030*, 2019.
- Baratin, A., George, T., Laurent, C., Hjelm, R. D., Lajoie, G., Vincent, P., and Lacoste-Julien, S. Implicit regularization via neural feature alignment. In *International Conference on Artificial Intelligence and Statistics*, pp. 2269–2277. PMLR, 2021.
- Chen, A. M., Lu, H.-m., and Hecht-Nielsen, R. On the geometry of feedforward neural network error surfaces. *Neural computation*, 5(6):910–927, 1993.
- Cheng, X. and Bartlett, P. Convergence of langevin mcmc in kl-divergence. In *Algorithmic Learning Theory*, pp. 186–211. PMLR, 2018.
- Cho, Y. and Saul, L. K. Kernel methods for deep learning. In *NIPS*, pp. 342–350. Curran Associates, Inc., 2009.
- Entezari, R., Sedghi, H., Saukh, O., and Neyshabur, B. The role of permutation invariance in linear mode connectivity of neural networks. *arXiv preprint arXiv:2110.06296*, 2021.
- Gal, Y. and Ghahramani, Z. Dropout as a Bayesian approximation: Representing model uncertainty in deep learning. In *Proceedings of the 33rd International Conference on Machine Learning (ICML-16)*, 2016.
- Garipov, T., Izmailov, P., Podoprikin, D., Vetrov, D. P., and Wilson, A. G. Loss surfaces, mode connectivity, and fast ensembling of dnns. In *NeurIPS*, pp. 8803–8812, 2018.
- Goodfellow, I., Bengio, Y., and Courville, A. *Deep learning*. MIT press, 2016.
- Halverson, J., Maiti, A., and Stoner, K. Neural networks and quantum field theory. *Machine Learning: Science and Technology*, 2(3):035002, 2021.
- Hofmann, T., Schölkopf, B., and Smola, A. J. Kernel methods in machine learning. *The annals of statistics*, pp. 1171–1220, 2008.
- Horn, R. A. and Johnson, C. R. *Matrix analysis*. Cambridge university press, 2012.
- Horn, R. A., Horn, R. A., and Johnson, C. R. *Topics in matrix analysis*. Cambridge university press, 1994.
- Hron, J., Bahri, Y., Novak, R., Pennington, J., and Sohl-Dickstein, J. Exact posterior distributions of wide bayesian neural networks. *arXiv preprint arXiv:2006.10541*, 2020.
- Kingma, D. P. and Ba, J. Adam: A method for stochastic optimization. *arXiv preprint arXiv:1412.6980*, 2014.
- Krizhevsky, A., Sutskever, I., and Hinton, G. E. Imagenet classification with deep convolutional neural networks. In *NIPS*, pp. 1106–1114, 2012.
- Lee, J., Bahri, Y., Novak, R., Schoenholz, S. S., Pennington, J., and Sohl-Dickstein, J. Deep neural networks as gaussian processes. *arXiv preprint arXiv:1711.00165*, 2017.
- Li, Q. and Sompolinsky, H. Statistical mechanics of deep linear neural networks: The back-propagating renormalization group. *arXiv preprint arXiv:2012.04030*, 2020.

- Lou, Y., Mingard, C., and Hayou, S. The equilibrium hypothesis: Rethinking implicit regularization in deep neural networks, 2021.
- MacKay, D. J. C. A practical bayesian framework for backpropagation networks. *Neural Comput.*, 4(3): 448–472, 1992.
- Matthews, A. G. d. G., Rowland, M., Hron, J., Turner, R. E., and Ghahramani, Z. Gaussian process behaviour in wide deep neural networks. *arXiv preprint arXiv:1804.11271*, 2018.
- Naveh, G. and Ringel, Z. A self consistent theory of gaussian processes captures feature learning effects in finite cnns. *arXiv preprint arXiv:2106.04110*, 2021.
- Naveh, G., Ben-David, O., Sompolinsky, H., and Ringel, Z. Predicting the outputs of finite networks trained with noisy gradients. *arXiv preprint arXiv:2004.01190*, 2020.
- Ober, S. W. and Aitchison, L. A variational approximate posterior for the deep wishart process. *arXiv preprint arXiv:2107.10125*, 2021.
- Roberts, D. A., Yaida, S., and Hanin, B. The principles of deep learning theory. *arXiv preprint arXiv:2106.10165*, 2021.
- Roberts, G. O. and Tweedie, R. L. Exponential convergence of langevin distributions and their discrete approximations. *Bernoulli*, pp. 341–363, 1996.
- Salimbeni, H. and Deisenroth, M. Doubly stochastic variational inference for deep gaussian processes. *arXiv preprint arXiv:1705.08933*, 2017.
- Shawe-Taylor, J. and Cristianini, N. *Kernel methods for pattern analysis*. Cambridge university press, 2004.
- Smola, A. J. and Schölkopf, B. *Learning with kernels*. MIT Press, 1998.
- Wu, C., Masoomi, A., Gretton, A., and Dy, J. Deep layer-wise networks have closed-form weights. *arXiv preprint arXiv:2202.01210*, 2022.
- Yaida, S. Non-gaussian processes and neural networks at finite widths. In *Mathematical and Scientific Machine Learning*, pp. 165–192. PMLR, 2020.
- Yang, G. and Hu, E. J. Feature learning in infinite-width neural networks. *arXiv preprint arXiv:2011.14522*, 2020.
- Zavatone-Veth, J. and Pehlevan, C. Exact marginal prior distributions of finite bayesian neural networks. *Advances in Neural Information Processing Systems*, 34, 2021.
- Zavatone-Veth, J. A., Canatar, A., and Pehlevan, C. Asymptotics of representation learning in finite bayesian neural networks. *arXiv preprint arXiv:2106.00651*, 2021.

A Optimizing the deep kernel machine objective is equivalent to Langevin sampling

We consider Langevin sampling on the deep Gaussian process model discussed in Sec. 3.1. The deep kernel process paper (Aitchison et al., 2020) emphasises that the features at layer ℓ , denoted $\mathbf{F}_\ell \in \mathbb{R}^{P \times N_\ell}$, depend only on the Gram matrix at the previous and next layers, $\mathbf{G}_{\ell-1}$ and $\mathbf{G}_{\ell+1}$, and not on the features at those layers. To infer \mathbf{F}_ℓ , we use the joint log-probability,

$$\mathcal{J} = \sum_{\ell=1}^{L+1} \log P(\mathbf{F}_\ell | \mathbf{F}_{\ell-1}) \quad (45)$$

selecting out terms that depend on \mathbf{F}_ℓ (or equivalently \mathbf{G}_ℓ),

$$= \log P(\mathbf{F}_\ell | \mathbf{F}_{\ell-1}) + \log P(\mathbf{F}_{\ell+1} | \mathbf{F}_\ell) \quad (46)$$

and remembering that $\log P(\mathbf{F}_\ell | \mathbf{F}_{\ell-1})$ can be written entirely in terms of Gram matrices,

$$= -\frac{N_\ell}{2} \text{tr}(\mathbf{G}_\ell \mathbf{K}^{-1}(\mathbf{G}_{\ell-1})) + \log P(\mathbf{F}_{\ell+1} | \mathbf{F}_\ell) + \text{const}. \quad (47)$$

Now, we consider doing Langevin sampling for \mathbf{F}_ℓ ,

$$d\mathbf{F}_\ell = \frac{1}{2} dt \frac{\partial \mathcal{J}}{\partial \mathbf{F}_\ell} + d\mathbf{\Xi}, \quad (48)$$

where $d\mathbf{\Xi} \in \mathbb{R}^{P \times N_\ell}$ can be understood as IID Gaussian noise (formally, it is the differential of a matrix-valued Wiener process). Thus, update to \mathbf{G} can be written, (note that the $d\mathbf{F}_\ell d\mathbf{F}_\ell^T$ can't be neglected as $d\mathbf{F}_\ell$ contains a Wiener process),

$$d\mathbf{G}_\ell = \frac{1}{N_\ell} d(\mathbf{F}_\ell \mathbf{F}_\ell^T) = \frac{1}{N_\ell} (d\mathbf{F}_\ell \mathbf{F}_\ell^T + \mathbf{F}_\ell d\mathbf{F}_\ell^T + d\mathbf{F}_\ell d\mathbf{F}_\ell^T) \quad (49)$$

$$= \frac{1}{2N_\ell} dt \left(\left(\frac{\partial \mathcal{J}}{\partial \mathbf{F}_\ell} \right) \mathbf{F}_\ell^T + \mathbf{F}_\ell \left(\frac{\partial \mathcal{J}}{\partial \mathbf{F}_\ell} \right)^T \right) + \frac{1}{N_\ell} (d\mathbf{\Xi} \mathbf{F}_\ell^T + \mathbf{F}_\ell d\mathbf{\Xi}^T) + \frac{1}{N_\ell} d\mathbf{\Xi} d\mathbf{\Xi}^T. \quad (50)$$

Now, we consider all of the stochastic terms, and show that in the infinite width limit, they are deterministic and equal to their expectation. First, we consider $d\mathbf{\Xi} d\mathbf{\Xi}^T$. Remembering that $\mathbf{\Xi} \in \mathbb{R}^{P \times N_\ell}$, the last term can be understood as an average of N_ℓ outer products,

$$\frac{1}{N_\ell} d\mathbf{\Xi} d\mathbf{\Xi}^T = \frac{1}{N_\ell} \sum_{\lambda=1}^{N_\ell} d\boldsymbol{\xi}_\lambda d\boldsymbol{\xi}_\lambda^T \quad (51)$$

where $\mathbf{\Xi} = (\boldsymbol{\xi}_1, \dots, \boldsymbol{\xi}_{N_\ell})$. Taking the limit as the number of intermediate layer features goes to infinity, $N_\ell \rightarrow \infty$, and remembering that $\boldsymbol{\xi}_\lambda$ are IID for different λ , the law of large numbers tells us that this term becomes deterministic and equal to its expectation,

$$\lim_{N_\ell \rightarrow \infty} \frac{1}{N_\ell} d\mathbf{\Xi} d\mathbf{\Xi}^T = \mathbb{E} \left[d\boldsymbol{\xi}_\lambda d\boldsymbol{\xi}_\lambda^T \right] = dt \mathbf{I}, \quad (52)$$

Next, consider an element of $\mathbf{F}_\ell d\mathbf{\Xi}$, which is Gaussian, as it is the sum of Gaussian elements in $d\mathbf{\Xi}$, which are IID with variance dt ,

$$\frac{1}{N_\ell} \sum_{\lambda=1}^{N_\ell} F_{i\lambda}^\ell d\Xi_{k\lambda} \sim \mathcal{N}(0, dt v_i) \quad (53)$$

The variance is,

$$v_i = \frac{1}{N_\ell^2} \sum_{\lambda=1}^{N_\ell} (F_{i\lambda}^\ell)^2 = \frac{1}{N_\ell} G_{ii}^\ell \quad (54)$$

Thus, the variance goes to zero in the infinite limit,

$$\lim_{N_\ell \rightarrow \infty} v_i = \lim_{N_\ell \rightarrow \infty} \frac{1}{N_\ell} G_{ii}^\ell = 0 \quad (55)$$

Thus,

$$\lim_{N_\ell \rightarrow \infty} \frac{1}{N_\ell} \sum_{\lambda=1}^{N_\ell} F_{i\lambda}^\ell d\Xi_{k\lambda} = 0. \quad (56)$$

Substituting these results into Eq. (50), and taking the limit $N_\ell \rightarrow \infty$ as given, $d\mathbf{G}_\ell$ becomes deterministic, allowing us to write, the dynamics under a Langevin diffusion as,

$$\dot{\mathbf{G}}_\ell = \frac{1}{2N_\ell} \left(\left(\frac{\partial \mathcal{J}}{\partial \mathbf{F}_\ell} \right) \mathbf{F}_\ell^T + \mathbf{F}_\ell \left(\frac{\partial \mathcal{J}}{\partial \mathbf{F}_\ell} \right)^T \right) + \mathbf{I}. \quad (57)$$

Now, our goal is to rewrite this expression entirely in terms of \mathbf{G}_ℓ . As such, we write $\frac{\partial \mathcal{J}}{\partial \mathbf{F}_\ell}$ in terms of $\frac{\partial \mathcal{J}}{\partial \mathbf{G}_\ell}$,

$$\frac{\partial \mathcal{J}}{\partial F_{\alpha\beta}^\ell} = \sum_{ij} \frac{\partial \mathcal{J}}{\partial G_{ij}^\ell} \frac{\partial G_{ij}^\ell}{\partial F_{\alpha\beta}^\ell} \quad (58)$$

$$= \frac{1}{N_\ell} \sum_{ij} \frac{\partial \mathcal{J}}{\partial G_{ij}^\ell} \frac{\partial}{\partial F_{\alpha\beta}^\ell} \sum_k F_{ik}^\ell F_{jk}^\ell \quad (59)$$

$$= \frac{1}{N_\ell} \sum_{ij} \frac{\partial \mathcal{J}}{\partial G_{ij}^\ell} \frac{\partial}{\partial F_{\alpha\beta}^\ell} \sum_k (\delta_{\alpha i} \delta_{\beta k} F_{jk}^\ell + F_{ik}^\ell \delta_{\alpha j} \delta_{\beta k}) \quad (60)$$

$$= \frac{1}{N_\ell} \left(\sum_j \frac{\partial \mathcal{J}}{\partial G_{\alpha j}^\ell} F_{j\beta}^\ell + \sum_i \frac{\partial \mathcal{J}}{\partial G_{i\alpha}^\ell} F_{i\beta}^\ell \right), \quad (61)$$

As the gradient of \mathcal{J} wrt \mathbf{G} is symmetric,

$$\frac{\partial \mathcal{J}}{\partial \mathbf{F}_\ell} = \frac{2}{N_\ell} \frac{\partial \mathcal{J}}{\partial \mathbf{G}} \mathbf{F}_\ell. \quad (62)$$

Thus, we can rewrite the expected updates for \mathbf{G}_ℓ entirely in terms of \mathbf{G}_ℓ and not in terms of \mathbf{F}_ℓ ,

$$\dot{\mathbf{G}}_\ell = \frac{1}{N_\ell^2} \left(\frac{\partial \mathcal{J}}{\partial \mathbf{G}_\ell} \mathbf{F}_\ell \mathbf{F}_\ell^T + \mathbf{F}_\ell \mathbf{F}_\ell^T \frac{\partial \mathcal{J}}{\partial \mathbf{G}_\ell} \right) + \mathbf{I} \quad (63)$$

$$\dot{\mathbf{G}}_\ell = \frac{1}{N_\ell} \left(\frac{\partial \mathcal{J}}{\partial \mathbf{G}_\ell} \mathbf{G}_\ell + \mathbf{G}_\ell \frac{\partial \mathcal{J}}{\partial \mathbf{G}_\ell} \right) + \mathbf{I}. \quad (64)$$

Now, we seek to interpret these expected Langevin dynamics as preconditioned gradient descent under a modified loss. Remembering that \mathbf{G}_ℓ is full rank as we have sent $N_\ell \rightarrow \infty$, it makes sense to consider the following objective,

$$N\mathcal{L} = \mathcal{J} + \frac{N_\ell}{2} \log |\mathbf{G}_\ell| \quad (65)$$

$$\frac{\partial (N\mathcal{L})}{\partial \mathbf{G}_\ell} = \frac{\partial \mathcal{J}}{\partial \mathbf{G}_\ell} + \frac{N_\ell}{2} \mathbf{G}_\ell^{-1}, \quad (66)$$

We then precondition using the positive definite matrix, $\frac{1}{N_\ell} (\mathbf{G}_\ell \otimes \mathbf{I} + \mathbf{I} \otimes \mathbf{G}_\ell)$, where \otimes is the Kronecker product, and $\text{vec}(\cdot)$ takes all elements of a matrix, and rearranges them to form a vector,

$$\frac{1}{N_\ell} (\mathbf{G}_\ell \otimes \mathbf{I} + \mathbf{I} \otimes \mathbf{G}_\ell) \text{vec} \left(\frac{\partial (N\mathcal{L})}{\partial \mathbf{G}_\ell} \right) = (\mathbf{G}_\ell \otimes \mathbf{I} + \mathbf{I} \otimes \mathbf{G}_\ell) \text{vec} \left(\frac{1}{N_\ell} \frac{\partial \mathcal{J}}{\partial \mathbf{G}_\ell} + \frac{1}{2} \mathbf{G}_\ell^{-1} \right) \quad (67)$$

$$= \text{vec} \left(\frac{1}{N_\ell} \left(\frac{\partial \mathcal{J}}{\partial \mathbf{G}_\ell} \mathbf{G}_\ell + \mathbf{G}_\ell \frac{\partial \mathcal{J}}{\partial \mathbf{G}_\ell} \right) + \mathbf{I} \right). \quad (68)$$

This expression matches the dynamics under Langevin sampling (Eq. 64), so preconditioned gradient descent on \mathcal{L} (Eq. 65) is equivalent to the dynamics on \mathbf{G}_ℓ induced by a Langevin diffusion.

The \mathbf{G}_ℓ dependent terms in the full objective are thus,

$$N\mathcal{L} = \frac{N_\ell}{2} (\log |\mathbf{G}_\ell| - \text{tr} (\mathbf{K}^{-1} (\mathbf{G}_{\ell-1}) \mathbf{G}_\ell)) + \log P (\mathbf{F}_{\ell+1}|\mathbf{F}_\ell) + \text{const} \quad (69)$$

$$= \frac{N_\ell}{2} \log |\mathbf{G}_\ell| + \log P (\mathbf{F}_{\ell+1}|\mathbf{F}_\ell) + \log P (\mathbf{F}_\ell|\mathbf{F}_{\ell-1}) + \text{const} \quad (70)$$

$$= \frac{N_\ell}{2} \log |\mathbf{G}_\ell| + \sum_{\ell=1}^{L+1} \log P (\mathbf{F}_\ell|\mathbf{F}_{\ell-1}) + \text{const} \quad (71)$$

Generalising to all layers, we obtain,

$$N\mathcal{L} = \sum_{\ell=1}^{L+1} \left(\frac{N_\ell}{2} \log |\mathbf{G}_\ell| + \log P (\mathbf{F}_\ell|\mathbf{F}_{\ell-1}) \right). \quad (72)$$

As this becomes infinite when $N \rightarrow \infty$, we obtain the objective in the main text (Eq. 22) by dividing both sides by N .

B Technical considerations for neural networks

For isotropic kernels, the kernel can be directly written as a function of \mathbf{G}_ℓ without further assumptions (Eq. (8)), and as the Langevin sampling section (Appendix A) directly describes the evolution of Gram matrices exact inference is possible.

However, the forms for the kernel in Cho & Saul (2009) for a network using e.g. relu nonlinearities (Eq. 13) do require additional assumptions. In particular, their expressions are only correct if the features, \mathbf{F}_ℓ , are Gaussian. While this is true a-priori, it is not necessarily true a-posteriori. In particular, the concern is that Langevin sampling might give non-Gaussian features, \mathbf{F}_ℓ , albeit with known Gram matrix, \mathbf{G}_ℓ . And that would imply that $\frac{1}{N_\ell} \phi(\mathbf{F}_\ell) \phi^T(\mathbf{F}_\ell) \neq \mathbf{K}(\mathbf{G}_\ell)$, where $\mathbf{K}(\mathbf{G}_\ell)$ is one of the expressions given by Cho & Saul (2009). This is not an issue for variational formulation, as we explicitly consider Gaussian approximate posteriors (Eq. 19), but variational inference is not necessarily exact. To fix this issue, we need to ensure that the features entering the nonlinearity really are Gaussian. This can be achieved by blowing up to an even larger width before going through the nonlinearity. In particular, the network becomes,

$$\mathbf{F}_{\ell+1} = \phi(\mathbf{H}_\ell) \mathbf{U}_\ell \quad (73)$$

$$\mathbf{H}_\ell = \mathbf{F}_\ell \mathbf{V}_\ell \quad (74)$$

where \mathbf{U}_ℓ and \mathbf{V}_ℓ are weight matrices,

$$\mathbf{U}_\ell \in \mathbb{R}^{M_\ell \times N_\ell} \quad \mathbf{U}_{\lambda\mu}^\ell \sim \mathcal{N} \left(0, \frac{1}{M_\ell} \right) \quad (75)$$

$$\mathbf{V}_\ell \in \mathbb{R}^{N_\ell \times M_\ell} \quad \mathbf{V}_{\lambda\mu}^\ell \sim \mathcal{N} \left(0, \frac{1}{N_\ell} \right) \quad (76)$$

$$\mathbf{H}_\ell \in \mathbb{R}^{P \times M_\ell}. \quad (77)$$

All that's happening is that before going through the nonlinearity, we do another linear mapping that blows up the dimension to M_ℓ . We take,

$$M_\ell = MN_\ell \quad (78)$$

and $M \rightarrow \infty$. Critically, this implies that,

$$P (\mathbf{H}_\ell|\mathbf{F}_\ell) = \prod_{\lambda=1}^{M_\ell} \mathcal{N} (\mathbf{h}_\lambda^\ell; \mathbf{0}, \mathbf{G}_\ell). \quad (79)$$

and this holds *both* a-posteriori and a-priori (Lee et al., 2017; Matthews et al., 2018; Hron et al., 2020), because the width of \mathbf{H}_ℓ is infinitely larger than the width of $\mathbf{F}_{\ell+1}$. Thus, the features that go into the nonlinearity are always Gaussian (a-priori and a-posteriori) and the expressions given by Cho & Saul (2009) can always be used.

C Scaling deep kernel methods using inducing points

To do large-scale experiments on UCI datasets, we introduce inducing point deep kernel machines by extending Gaussian process inducing point methods (e.g. Salimbeni & Deisenroth, 2017) to the deep kernel machine setting. This approach uses the variational interpretation of the deep kernel machine objective described in the main text.

To do inducing-point variational inference, we need to explicitly introduce top-layer features, $\tilde{\mathbf{F}}_{L+1} \in \mathbb{R}^{P \times N_\ell}$,

$$\mathbb{P}(\tilde{\mathbf{F}}_{L+1} | \mathbf{F}_L) = \prod_{\lambda=1}^{N_\ell} \mathcal{N}(\tilde{\mathbf{f}}_\lambda^{L+1}; \mathbf{0}, \mathbf{K}_f(\mathbf{F}_L)), \quad (80)$$

$$\mathbb{P}(\tilde{\mathbf{Y}} | \tilde{\mathbf{F}}_{L+1}) = \prod_{\lambda=1}^{N_\ell} \mathcal{N}(\tilde{\mathbf{y}}_\lambda; \tilde{\mathbf{f}}_\lambda^{L+1}, \sigma^2 \mathbf{I}). \quad (81)$$

Here, $\tilde{\mathbf{F}}_{L+1}$ corresponds to the N copies of \mathbf{Y} in $\tilde{\mathbf{Y}}$. Remembering that the first ν_{L+1} columns of $\tilde{\mathbf{Y}}$ correspond to the original data, \mathbf{Y} , we can define $\mathbf{F}_{L+1} \in \mathbb{R}^{P \times \nu_{L+1}}$ as corresponding columns of $\tilde{\mathbf{F}}_{L+1}$, i.e.

$$\mathbf{Y} = (\tilde{\mathbf{y}}_1 \quad \dots \quad \tilde{\mathbf{y}}_{\nu_{L+1}}) \quad \mathbf{F}_{L+1} = (\tilde{\mathbf{f}}_1^{L+1} \quad \dots \quad \tilde{\mathbf{f}}_{\nu_{L+1}}^{L+1}). \quad (82)$$

Further, we separate $\mathbf{F}_\ell \in \mathbb{R}^{N_\ell \times (P_i + P_t)}$ into the inducing features, $\mathbf{F}_i^\ell \in \mathbb{R}^{N_\ell \times P_i}$ and the test/train features, $\mathbf{F}_t^\ell \in \mathbb{R}^{N_\ell \times P_t}$, where P_i is the number of inducing points and P_t is the number of test/train points. Likewise, we separate the inputs, \mathbf{X} , and outputs, \mathbf{Y} , into (potentially trained) inducing inputs, \mathbf{X}_i , and trained inducing outputs, \mathbf{Y}_i , and the real test/training inputs, \mathbf{X}_t , and outputs, \mathbf{Y}_t ,

$$\mathbf{F}_\ell = \begin{pmatrix} \mathbf{F}_i^\ell \\ \mathbf{F}_t^\ell \end{pmatrix} \quad \tilde{\mathbf{F}}_{L+1} = \begin{pmatrix} \tilde{\mathbf{F}}_i^{L+1} \\ \tilde{\mathbf{F}}_t^{L+1} \end{pmatrix} \quad \mathbf{X} = \begin{pmatrix} \mathbf{X}_i \\ \mathbf{X}_t \end{pmatrix} \quad \mathbf{Y} = \begin{pmatrix} \mathbf{Y}_i \\ \mathbf{Y}_t \end{pmatrix} \quad \tilde{\mathbf{Y}} = \begin{pmatrix} \tilde{\mathbf{Y}}_i \\ \tilde{\mathbf{Y}}_t \end{pmatrix} \quad (83)$$

We follow the usual doubly stochastic inducing point approach for DGPs. In particular, we treat all the features at intermediate layers, $\mathbf{F}_1, \dots, \mathbf{F}_L$, and the top-layer train/test features, \mathbf{F}_t^{L+1} as latent variables. However, we deviate from the usual setup in treating the top-layer inducing outputs, \mathbf{F}_i^{L+1} , as learned parameters and maximize over them to ensure that the ultimate method does not require sampling, and at the same time allows minibatched training. The prior and approximate posterior factorise across layers, and the approximate posterior distribution over \mathbf{F}_t^{L+1} is given by the conditional prior, so those terms will cancel when we come to the ELBO,

$$\mathbb{Q}(\mathbf{F}_1, \dots, \mathbf{F}_L, \tilde{\mathbf{F}}_t^{L+1} | \mathbf{X}, \mathbf{F}_i^{L+1}) = \mathbb{P}(\tilde{\mathbf{F}}_t^{L+1} | \mathbf{F}_i^{L+1}, \mathbf{G}_L) \prod_{\ell=1}^{L+1} \mathbb{Q}(\mathbf{F}_i^\ell, \mathbf{F}_t^\ell | \mathbf{G}_{\ell-1}), \quad (84a)$$

$$\mathbb{P}(\mathbf{F}_1, \dots, \mathbf{F}_L, \tilde{\mathbf{F}}_t^{L+1} | \mathbf{X}, \mathbf{F}_i^{L+1}) = \mathbb{P}(\tilde{\mathbf{F}}_t^{L+1} | \mathbf{F}_i^{L+1}, \mathbf{G}_L) \prod_{\ell=1}^{L+1} \mathbb{P}(\mathbf{F}_i^\ell, \mathbf{F}_t^\ell | \mathbf{G}_{\ell-1}), \quad (84b)$$

where,

$$\mathbf{G}_{\ell-1} = \frac{1}{N_{\ell-1}} \mathbf{F}_{\ell-1} \mathbf{F}_{\ell-1}^T = \begin{pmatrix} \mathbf{F}_i^{\ell-1} (\mathbf{F}_i^{\ell-1})^T & \mathbf{F}_i^{\ell-1} (\mathbf{F}_t^{\ell-1})^T \\ \mathbf{F}_t^{\ell-1} (\mathbf{F}_i^{\ell-1})^T & \mathbf{F}_t^{\ell-1} (\mathbf{F}_t^{\ell-1})^T \end{pmatrix} \quad (85)$$

and remember $\mathbf{F}_0 = \mathbf{X}$, so $\mathbf{G}_0 = \frac{1}{N_0} \mathbf{X} \mathbf{X}^T$. The prior and approximate posterior at each layer factorises into a distribution over the inducing points and a distribution over the test/train points,

$$\mathbb{Q}(\mathbf{F}_i^\ell, \mathbf{F}_t^\ell | \mathbf{G}_{\ell-1}) = \mathbb{P}(\mathbf{F}_t^\ell | \mathbf{F}_i^\ell, \mathbf{G}_{\ell-1}) \mathbb{Q}(\mathbf{F}_i^\ell), \quad (86a)$$

$$\mathbb{P}(\mathbf{F}_i^\ell, \mathbf{F}_t^\ell | \mathbf{G}_{\ell-1}) = \mathbb{P}(\mathbf{F}_t^\ell | \mathbf{F}_i^\ell, \mathbf{G}_{\ell-1}) \mathbb{P}(\mathbf{F}_i^\ell | \mathbf{G}_{\ell-1}). \quad (86b)$$

Critically, the approximate posterior samples the test/train points from the conditional prior, which is going to lead to cancellation when we compute the ELBO. Concretely, the prior approximate posterior over inducing points are given by,

$$\mathbb{Q}(\mathbf{F}_i^\ell) = \mathcal{N}(\mathbf{f}_{i;\lambda}^\ell; \mathbf{0}, \mathbf{G}_{ii}^\ell), \quad (87a)$$

$$\mathbb{P}(\mathbf{F}_i^\ell | \mathbf{F}_{\ell-1}) = \mathcal{N}(\mathbf{f}_{i;\lambda}^\ell; \mathbf{0}, \mathbf{K}(\mathbf{G}_{ii}^{\ell-1})) \quad (87b)$$

The approximate posterior is directly analogous to Eq. (19) and the prior is directly analogous to Eq. (1), but where we have specified that this is only over inducing points, and where we have where we have exploited the

infinite limit, which ensures that the approximate posterior covariance is equal to the Gram matrix (Eq. 18). Now we compute the ELBO (as the $P(\mathbf{F}_t^\ell | \mathbf{F}_i^\ell, \mathbf{G}_{\ell-1})$ terms are going to cancel in the ELBO, we consider them below when we come to describing sampling),

$$\begin{aligned} \text{ELBO}(\mathbf{F}_i^{L+1}, \mathbf{G}_1, \dots, \mathbf{G}_L) & \\ &= \mathbb{E}_{\mathbf{Q}(\mathbf{F}_1, \dots, \mathbf{F}_L, \tilde{\mathbf{F}}_t^{L+1} | \mathbf{X}, \mathbf{F}_i^{L+1})} \left[\log P(\tilde{\mathbf{Y}}_t | \tilde{\mathbf{F}}_t^{L+1}, \mathbf{G}_L) + \log \frac{P(\mathbf{F}_1, \dots, \mathbf{F}_L, \tilde{\mathbf{F}}_t^{L+1} | \mathbf{X}, \mathbf{F}_i^{L+1})}{Q(\mathbf{F}_1, \dots, \mathbf{F}_L, \tilde{\mathbf{F}}_t^{L+1} | \mathbf{X}, \mathbf{F}_i^{L+1})} \right] \end{aligned} \quad (88)$$

substituting Eq. (84) and Eq. (86) and cancelling $P(\tilde{\mathbf{F}}_t^\ell | \mathbf{F}_i^\ell, \mathbf{G}_{\ell-1})$

$$\text{ELBO}(\mathbf{F}_i^{L+1}, \mathbf{G}_1, \dots, \mathbf{G}_L) = \mathbb{E}_{\mathbf{Q}(\mathbf{F}_1, \dots, \mathbf{F}_L, \tilde{\mathbf{F}}_t^{L+1} | \mathbf{X}, \mathbf{F}_i^{L+1})} \left[\log P(\tilde{\mathbf{Y}}_t | \tilde{\mathbf{F}}_t^{L+1}, \mathbf{G}_L) + \sum_{\ell=1}^L \log \frac{P(\mathbf{F}_i^\ell | \mathbf{G}_{\ell-1})}{Q(\mathbf{F}_i^\ell)} \right]. \quad (89)$$

In the infinite limit, the Gram matrices become deterministic by the law of large numbers (Eq. 18), and we know that $P(\mathbf{F}_i^\ell | \mathbf{G}_{\ell-1})$ and $Q(\mathbf{F}_i^\ell)$ can be written in terms of only the Gram matrices (Eq. 10). Thus, the ELBO becomes,

$$\text{ELBO}(\mathbf{F}_i^{L+1}, \mathbf{G}_1, \dots, \mathbf{G}_L) = \mathbb{E}_{\mathbf{Q}(\tilde{\mathbf{F}}_t^{L+1} | \mathbf{F}_i^{L+1}, \mathbf{G}_L)} [\log P(\tilde{\mathbf{Y}}_t | \tilde{\mathbf{F}}_t^{L+1}, \mathbf{G}_L)] + \sum_{\ell=1}^L \log \frac{P(\mathbf{F}_i^\ell | \mathbf{G}_{\ell-1})}{Q(\mathbf{F}_i^\ell)}. \quad (90)$$

And to obtain our final scalable object, we again divide by N to ensure that it remains finite in the infinite limit,

$$\mathcal{L}_{\text{ind}}(\mathbf{F}_i^{L+1}, \mathbf{G}_{\text{ii}}^1, \dots, \mathbf{G}_{\text{ii}}^L) = \mathbb{E}_{\mathbf{Q}(\mathbf{F}_t^{L+1} | \mathbf{F}_i^{L+1}, \mathbf{G}_L)} [\log P(\mathbf{Y}_t | \mathbf{F}_t^{L+1}, \mathbf{G}_L)] + \frac{1}{N} \sum_{\ell=1}^L \log \frac{P(\mathbf{F}_i^\ell | \mathbf{G}_{\ell-1})}{Q(\mathbf{F}_i^\ell)}, \quad (91)$$

The second term, is exactly the same as in the deep kernel machine objective (Eq. 24), applied only the inducing points. The first term is obtained by taking the separate ‘‘copies’’ of \mathbf{F}_t^{L+1} as IID in the approximate posterior over $\tilde{\mathbf{F}}_t^{L+1}$,

$$\mathbb{E}_{\mathbf{Q}(\tilde{\mathbf{F}}_t^{L+1} | \mathbf{F}_i^{L+1}, \mathbf{G}_L)} [\log P(\tilde{\mathbf{Y}}_t | \tilde{\mathbf{F}}_t^{L+1}, \mathbf{G}_L)] = N \mathbb{E}_{\mathbf{Q}(\mathbf{F}_t^{L+1} | \mathbf{F}_i^{L+1}, \mathbf{G}_L)} [\log P(\mathbf{Y}_t | \mathbf{F}_t, \mathbf{G}_L)]. \quad (92)$$

Now that we have a simple form for the ELBO, we need to compute the expected likelihood, $\mathbb{E}_{\mathbf{Q}(\mathbf{F}_t^{L+1} | \mathbf{F}_i^{L+1}, \mathbf{G}_L)} [\log P(\mathbf{Y}_t | \mathbf{F}_t^{L+1}, \mathbf{G}_L)]$ by sampling the full Gram matrices, including test/train points, conditioned on the optimized inducing Gram matrices. We start by defining the full Gram matrix,

$$\mathbf{G}_\ell = \begin{pmatrix} \mathbf{G}_{\text{ii}}^\ell & \mathbf{G}_{\text{it}}^\ell \\ \mathbf{G}_{\text{ti}}^\ell & \mathbf{G}_{\text{tt}}^\ell \end{pmatrix} \quad (93)$$

for both inducing points (labelled ‘‘i’’) and test/training points (labelled ‘‘t’’) from just $\mathbf{G}_{\text{ii}}^\ell$. For clarity, we have $\mathbf{G}_\ell \in \mathbb{R}^{P \times P}$, $\mathbf{G}_{\text{ii}}^\ell \in \mathbb{R}^{P_i \times P_i}$, $\mathbf{G}_{\text{ti}}^\ell \in \mathbb{R}^{P_t \times P_i}$, $\mathbf{G}_{\text{tt}}^\ell \in \mathbb{R}^{P_t \times P_t}$, where P_i is the number of inducing points, P_t is the number of train/test points and $P = P_i + P_t$ is the total number of inducing and train/test points.

The conditional distribution over \mathbf{F}_t^ℓ given \mathbf{F}_i^ℓ is,

$$P(\mathbf{F}_t^\ell | \mathbf{F}_i^\ell, \mathbf{G}_{\ell-1}) = \prod_{\lambda=1}^{N_\ell} \mathcal{N}(\mathbf{f}_{t;\lambda}^\ell; \mathbf{K}_{\text{ti}} \mathbf{K}_{\text{ii}}^{-1} \mathbf{f}_{i;\lambda}^\ell, \mathbf{K}_{\text{tt-i}}) \quad (94)$$

where $\mathbf{f}_{t;\lambda}^\ell$ is the activation of the λ th feature for all train/test inputs, $\mathbf{f}_{i;\lambda}^\ell$ is the activation of the λ th feature for all train/test inputs, and $\mathbf{f}_{i;\lambda}^\ell$, and

$$\begin{pmatrix} \mathbf{K}_{\text{ii}} & \mathbf{K}_{\text{ti}}^T \\ \mathbf{K}_{\text{ti}} & \mathbf{K}_{\text{tt}} \end{pmatrix} = \mathbf{K} \begin{pmatrix} 1 & \\ & \frac{1}{N_{\ell-1}} \mathbf{F}_{\ell-1} \mathbf{F}_{\ell-1}^T \end{pmatrix} = \mathbf{K}(\mathbf{G}_{\ell-1}) \quad (95)$$

$$\mathbf{K}_{\text{tt-i}} = \mathbf{K}_{\text{tt}} - \mathbf{K}_{\text{ti}} \mathbf{K}_{\text{ii}}^{-1} \mathbf{K}_{\text{ti}}^T. \quad (96)$$

In the infinite limit, the Gram matrix becomes deterministic via the law of large numbers (as in Eq. 18), and as such \mathbf{G}_{it} and \mathbf{G}_{tt} become deterministic and equal to their expected values. Using Eq. (94), we can write,

$$\mathbf{F}_t^\ell = \mathbf{K}_{\text{ti}} \mathbf{K}_{\text{ii}}^{-1} \mathbf{F}_i^\ell + \mathbf{K}_{\text{tt-i}}^{1/2} \boldsymbol{\Xi}. \quad (97)$$

Algorithm 1 DKP prediction

Parameters: $\{\nu_\ell\}_{\ell=1}^L$
Optimized Gram matrices $\{\mathbf{G}_{ii}^\ell\}_{\ell=1}^L$
Inducing and train/test inputs: $\mathbf{X}_i, \mathbf{X}_t$
Inducing outputs: \mathbf{F}_i^{L+1}

Initialize full Gram matrix

$$\begin{pmatrix} \mathbf{G}_{ii}^0 & \mathbf{G}_{ti}^{0:T} \\ \mathbf{G}_{ti}^0 & \mathbf{G}_{tt}^0 \end{pmatrix} = \frac{1}{\nu_0} \begin{pmatrix} \mathbf{X}_i \mathbf{X}_i^T & \mathbf{X}_i \mathbf{X}_t^T \\ \mathbf{X}_t \mathbf{X}_i^T & \mathbf{X}_t \mathbf{X}_t^T \end{pmatrix}$$

Propagate full Gram matrix

for ℓ **in** $(1, \dots, L)$ **do**

$$\begin{pmatrix} \mathbf{K}_{ii} & \mathbf{K}_{ti}^T \\ \mathbf{K}_{ti} & \mathbf{K}_{tt} \end{pmatrix} = \mathbf{K} \left(\begin{pmatrix} \mathbf{G}_{ii}^{\ell-1} & (\mathbf{G}_{ti}^{\ell-1})^T \\ \mathbf{G}_{ti}^{\ell-1} & \mathbf{G}_{tt}^{\ell-1} \end{pmatrix} \right)$$

$$\mathbf{K}_{tt:i} = \mathbf{K}_{tt} - \mathbf{K}_{ti} \mathbf{K}_{ii}^{-1} \mathbf{K}_{ti}^T.$$

$$\mathbf{G}_{ti}^\ell = \mathbf{K}_{ti}^T \mathbf{K}_{ii}^{-1} \mathbf{G}_{ii}^\ell$$

$$\mathbf{G}_{tt}^\ell = \mathbf{K}_{ti}^T \mathbf{K}_{ii}^{-1} \mathbf{G}_{ii}^\ell \mathbf{K}_{ii}^{-1} \mathbf{K}_{ti} + \mathbf{K}_{tt:i}$$

end for

Final prediction using standard Gaussian process expressions

$$\begin{pmatrix} \mathbf{K}_{ii} & \mathbf{K}_{ti}^T \\ \mathbf{K}_{ti} & \mathbf{K}_{tt} \end{pmatrix} = \mathbf{K} \left(\begin{pmatrix} \mathbf{G}_{ii}^L & (\mathbf{G}_{ti}^L)^T \\ \mathbf{G}_{ti}^L & \mathbf{G}_{tt}^L \end{pmatrix} \right)$$

$$\mathbf{Y}_t \sim \mathcal{N}(\mathbf{K}_{ti} \mathbf{K}_{ii}^{-1} \mathbf{F}_i^{L+1}, \mathbf{K}_{tt} - \mathbf{K}_{ti} \mathbf{K}_{ii}^{-1} \mathbf{K}_{ti}^T + \sigma^2 \mathbf{I})$$

 where Ξ is a matrix with IID standard Gaussian elements. Thus,

$$\mathbf{G}_{ti}^\ell = \frac{1}{\nu} \mathbb{E} [\mathbf{F}_t^\ell (\mathbf{F}_i^\ell)^T] \tag{98}$$

$$= \frac{1}{\nu} \mathbf{K}_{ti} \mathbf{K}_{ii}^{-1} \mathbb{E} [\mathbf{F}_i^\ell (\mathbf{F}_i^\ell)^T] \tag{99}$$

$$= \mathbf{K}_{ti} \mathbf{K}_{ii}^{-1} \mathbf{G}_{ii}^\ell \tag{100}$$

and,

$$\mathbf{G}_{tt}^\ell = \frac{1}{\nu} \mathbb{E} [\mathbf{F}_t^\ell (\mathbf{F}_t^\ell)^T] \tag{101}$$

$$= \frac{1}{\nu} \mathbf{K}_{ti} \mathbf{K}_{ii}^{-1} \mathbb{E} [\mathbf{F}_i^\ell (\mathbf{F}_i^\ell)^T] \mathbf{K}_{ii}^{-1} \mathbf{K}_{ti}^T + \frac{1}{\nu} \mathbf{K}_{tt:i}^{1/2} \mathbb{E} [\Xi \Xi^T] \mathbf{K}_{tt:i}^{1/2} \tag{102}$$

$$= \mathbf{K}_{ti} \mathbf{K}_{ii}^{-1} \mathbf{G}_{ii}^\ell \mathbf{K}_{ii}^{-1} \mathbf{K}_{ti}^T + \mathbf{K}_{tt:i} \tag{103}$$

For the full prediction algorithm, see Alg. 1.

D Unimodality in linear deep kernel machines

 In the main text we showed that the deep kernel machine is unimodal when all ν_ℓ are equal. Here, we show that unimodality in linear DKMs also holds for all choices of ν_ℓ . Recall the linear DKM objective in Eq. (37),

$$\mathcal{L}(\mathbf{G}_1, \dots, \mathbf{G}_L) = \sum_{\ell=1}^{L+1} \frac{\nu_\ell}{2} (\log |\mathbf{G}_{\ell-1}^{-1} \mathbf{G}_\ell| - \text{Tr}(\mathbf{G}_{\ell-1}^{-1} \mathbf{G}_\ell)) \tag{104}$$

$$= \sum_{\ell=1}^{L+1} \frac{\nu_\ell}{2} (\log |\mathbf{G}_\ell| - \log |\mathbf{G}_{\ell-1}| - \text{Tr}(\mathbf{G}_{\ell-1}^{-1} \mathbf{G}_\ell)). \tag{105}$$

 To find the mode, again we set the gradient wrt \mathbf{G}_ℓ to zero,

$$\mathbf{0} = \frac{\partial \mathcal{L}}{\partial \mathbf{G}_\ell} = -\frac{\nu_{\ell+1} - \nu_\ell}{2} \mathbf{G}_\ell^{-1} - \frac{\nu_\ell}{2} \mathbf{G}_{\ell-1}^{-1} + \frac{\nu_{\ell+1}}{2} \mathbf{G}_\ell^{-1} \mathbf{G}_{\ell+1} \mathbf{G}_\ell^{-1}, \tag{106}$$

 for $\ell = 1, \dots, L$. Right multiplying by $2\mathbf{G}_\ell$ and rearranging,

$$\nu_{\ell+1} \mathbf{G}_\ell^{-1} \mathbf{G}_{\ell+1} = \nu_\ell \mathbf{G}_{\ell-1}^{-1} \mathbf{G}_\ell + (\nu_{\ell+1} - \nu_\ell) \mathbf{I}, \quad \text{for } \ell = 1, \dots, L. \tag{107}$$

 Evaluating this expression for $\ell = 1$ and $\ell = 2$, we gives,

$$\nu_2 \mathbf{G}_1^{-1} \mathbf{G}_2 = \nu_1 \mathbf{G}_0^{-1} \mathbf{G}_1 + (\nu_2 - \nu_1) \mathbf{I}, \tag{108}$$

$$\nu_3 \mathbf{G}_2^{-1} \mathbf{G}_3 = \nu_2 \mathbf{G}_1^{-1} \mathbf{G}_2 + (\nu_3 - \nu_2) \mathbf{I} = \nu_1 \mathbf{G}_0^{-1} \mathbf{G}_1 + (\nu_3 - \nu_1) \mathbf{I}. \tag{109}$$

Recurring, we get,

$$\nu_\ell \mathbf{G}_{\ell-1}^{-1} \mathbf{G}_\ell = \nu_1 \mathbf{G}_0^{-1} \mathbf{G}_1 + (\nu_\ell - \nu_1) \mathbf{I}. \quad (110)$$

Critically, this form highlights constraints on \mathbf{G}_1 . In particular, the right hand side, $\mathbf{G}_{\ell-1}^{-1} \mathbf{G}_\ell$, is the product of two positive definite matrices, so has positive eigenvalues (but may be non-symmetric Horn & Johnson, 2012). Thus, all eigenvalues of $\nu_1 \mathbf{G}_0^{-1} \mathbf{G}_1$ must be larger than $\nu_1 - \nu_\ell$, and this holds true at all layers. This will become important later, as it rules out spurious solutions.

Now, we can compute any \mathbf{G}_ℓ using,

$$\mathbf{G}_0^{-1} \mathbf{G}_\ell = \prod_{\ell'=1}^{\ell} (\mathbf{G}_{\ell'-1}^{-1} \mathbf{G}_{\ell'}) = \frac{1}{\prod_{\ell'=1}^{\ell} \nu_{\ell'}} \prod_{\ell'=1}^{\ell} (\nu_{\ell'} \mathbf{G}_{\ell'-1}^{-1} \mathbf{G}_{\ell'}) \quad (111)$$

$$\left(\prod_{\ell'=1}^{\ell} \nu_{\ell'} \right) \mathbf{G}_0^{-1} \mathbf{G}_\ell = \prod_{\ell'=1}^{\ell} (\nu_1 \mathbf{G}_0^{-1} \mathbf{G}_1 + (\nu_{\ell'} - \nu_1) \mathbf{I}) \quad (112)$$

This allows us to compute any \mathbf{G}_ℓ from just \mathbf{G}_0 and \mathbf{G}_1 . Now, we seek to solve for \mathbf{G}_1 using our knowledge of \mathbf{G}_{L+1} . Computing $\mathbf{G}_0^{-1} \mathbf{G}_{L+1}$,

$$\left(\prod_{\ell=1}^{L+1} \nu_\ell \right) \mathbf{G}_0^{-1} \mathbf{G}_{L+1} = \prod_{\ell=1}^{L+1} (\nu_1 \mathbf{G}_0^{-1} \mathbf{G}_1 + (\nu_\ell - \nu_1) \mathbf{I}). \quad (113)$$

We write the eigendecomposition of $\nu_1 \mathbf{G}_0^{-1} \mathbf{G}_1$ as,

$$\nu_1 \mathbf{G}_0^{-1} \mathbf{G}_1 = \mathbf{V} \mathbf{D} \mathbf{V}^{-1}. \quad (114)$$

Thus,

$$\left(\prod_{\ell=1}^{L+1} \nu_\ell \right) \mathbf{G}_0^{-1} \mathbf{G}_{L+1} = \prod_{\ell=1}^{L+1} (\mathbf{V} \mathbf{D} \mathbf{V}^{-1} + (\nu_\ell - \nu_1) \mathbf{I}) = \mathbf{V} \mathbf{\Lambda} \mathbf{V}^{-1} \quad (115)$$

where $\mathbf{\Lambda}$ is a diagonal matrix,

$$\mathbf{\Lambda} = \prod_{\ell=1}^{L+1} (\mathbf{D} + (\nu_\ell - \nu_1) \mathbf{I}). \quad (116)$$

Thus, we can identify \mathbf{V} and $\mathbf{\Lambda}$ by performing an eigendecomposition of the known matrix, $\left(\prod_{\ell=1}^{L+1} \nu_\ell \right) \mathbf{G}_0^{-1} \mathbf{G}_{L+1}$. Then, we can solve for \mathbf{D} (and hence \mathbf{G}_1) in terms of $\mathbf{\Lambda}$ and \mathbf{V} . The diagonal elements of \mathbf{D} satisfy,

$$0 = -\Lambda_{ii} + \prod_{k=1}^{L+1} (D_{ii} + (\nu_k - \nu_1)) \quad (117)$$

This is a polynomial, and remembering the constraints from Eq. (110), we are interested in solutions which satisfy,

$$\nu_1 - \nu_{\min} \leq D_{ii}. \quad (118)$$

where,

$$\nu_{\min} = \min(\nu_1, \dots, \nu_{L+1}) \quad (119)$$

To reason about the number of such solutions, we use Descartes' rule of signs, which states that the number of positive real roots is equal to or a multiple of two less than the number of sign changes in the coefficients of the polynomial. Thus, if there is one sign change, there must be one positive real root. For instance, in the following polynomial,

$$0 = x^3 + x^2 - 1 \quad (120)$$

the signs go as $(+), (+), (-)$, so there is only one sign change, and there is one real root. To use Descartes' rule of signs, we work in terms of D'_{ii} , which is constrained to be positive,

$$0 \leq D'_{ii} = D_{ii} - (\nu_1 - \nu_{\min}) \quad D_{ii} = D'_{ii} + (\nu_1 - \nu_{\min}). \quad (121)$$

Thus, the polynomial of interest (Eq. 117) becomes,

$$0 = -\Lambda_{ii} + \prod_{\ell=1}^{L+1} (D'_{ii} + (\nu_1 - \nu_{\min}) - (\nu_1 - \nu_{\ell})) = -\Lambda_{ii} + \prod_{\ell=1}^{L+1} (D'_{ii} + (\nu_{\ell} - \nu_{\min})) \quad (122)$$

where $0 < \nu_{\ell} - \nu_{\min}$ as ν_{\min} is defined to be the smallest ν_{ℓ} (Eq. 119). Thus, the constant term, $-\Lambda_{ii}$ is negative, while all other terms, $D'_{ii}, \dots, (D'_{ii})^{L+1}$ in the polynomial have positive coefficients. Thus, there is only one sign change, which proves the existence of only one valid real root, as required.

E Characterising the true posterior

Here, we use variational inference to reason about the form of the true posterior. In particular, we use entropy maximization arguments to show that, conditioned on \mathbf{G}_{ℓ} , the posterior over \mathbf{F}_{ℓ} is multivariate Gaussian and independent across features. Thus, the true posterior over \mathbf{F}_{ℓ} is a mixture of Gaussians with zero mean but different covariances, \mathbf{G}_{ℓ} . Finally, we show that the ELBO objective is convex in the distribution over $\mathbf{Q}(\mathbf{G}_1, \dots, \mathbf{G}_L)$.

First, we consider an the optimal approximate posterior over \mathbf{F}_{ℓ} , which is equal to the true posterior, conditioned on the Gram matrix, $\mathbf{G}_{\ell} = \frac{1}{N_{\ell}} \mathbf{F}_{\ell} \mathbf{F}_{\ell}^T$. We find the optimal approximate posterior takes on a simple, independent Gaussian form. In particular, all terms in the ELBO that depend on $\mathbf{Q}(\mathbf{F}_{\ell})$ are,

$$\mathcal{L} = \mathbb{E}_{\mathbf{Q}(\mathbf{F}_{\ell-1}, \mathbf{F}_{\ell}, \mathbf{F}_{\ell+1} | \mathbf{G}_{\ell})} [\log \mathbf{P}(\mathbf{F}_{\ell} | \mathbf{F}_{\ell-1}) + \log \mathbf{P}(\mathbf{F}_{\ell+1} | \mathbf{F}_{\ell})] + \mathbf{H}[\mathbf{Q}(\mathbf{F}_{\ell-1}, \mathbf{F}_{\ell}, \mathbf{F}_{\ell+1} | \mathbf{G}_{\ell})]. \quad (123)$$

Both $\log \mathbf{P}(\mathbf{F}_{\ell+1} | \mathbf{F}_{\ell})$ and $\log \mathbf{P}(\mathbf{F}_{\ell} | \mathbf{F}_{\ell-1})$ depend only on \mathbf{F}_{ℓ} only through \mathbf{G}_{ℓ} ,

$$\mathbb{E}_{\mathbf{Q}(\mathbf{F}_{\ell-1}, \mathbf{F}_{\ell})} [\log \mathbf{P}(\mathbf{F}_{\ell} | \mathbf{F}_{\ell-1})] = \frac{N_{\ell}}{2} (\mathbb{E}_{\mathbf{Q}(\mathbf{F}_{\ell-1})} [\log |\mathbf{K}^{-1}(\mathbf{G}_{\ell-1})|] - \text{tr}(\mathbb{E}_{\mathbf{Q}(\mathbf{F}_{\ell-1})} [\mathbf{K}^{-1}(\mathbf{G}_{\ell-1}) \mathbf{G}_{\ell}])) \quad (124)$$

$$\mathbb{E}_{\mathbf{Q}(\mathbf{F}_{\ell}, \mathbf{F}_{\ell+1})} [\log \mathbf{P}(\mathbf{F}_{\ell+1} | \mathbf{F}_{\ell})] = \frac{N_{\ell}}{2} (\log |\mathbf{K}^{-1}(\mathbf{G}_{\ell})| - \text{tr}(\mathbf{K}^{-1}(\mathbf{G}_{\ell}) \mathbb{E}_{\mathbf{Q}(\mathbf{F}_{\ell+1})} [\mathbf{G}_{\ell+1}])) \quad (125)$$

Thus, the optimal approximate posterior over \mathbf{F}_{ℓ} conditioned on all other latent variables, $\mathbf{Q}(\mathbf{F}_{\ell} | \mathbf{G}_{\ell})$, is determined entirely by the entropy term. By assumption, the Gram matrix is fixed, so the only relevant term in the ELBO is the entropy, and we know that the maximum entropy is achieved by taking \mathbf{F}_{ℓ} to be independent of $\mathbf{F}_{\ell-1}$ and $\mathbf{F}_{\ell+1}$ and to take each feature as independent Gaussian. The resulting distribution is,

$$\mathbf{P}(\mathbf{F}_{\ell} | \mathbf{G}_{\ell}) = \mathbf{Q}(\mathbf{F}_{\ell} | \mathbf{G}_{\ell}) = \prod_{\lambda=1}^{N_{\ell}} \mathcal{N}(\mathbf{f}_{\lambda}^{\ell}; \mathbf{0}, \mathbf{G}_{\ell}). \quad (126)$$

Thus, the optimal approximate posterior can be written as a mixture of Gaussians, where the mixture is over Gram matrices,

$$\mathbf{Q}(\mathbf{F}_1, \dots, \mathbf{F}_L) = \int d\mathbf{G}_1 \cdots d\mathbf{G}_L \mathbf{Q}(\mathbf{G}_1, \dots, \mathbf{G}_L) \prod_{\ell=1}^L \mathbf{Q}(\mathbf{F}_{\ell} | \mathbf{G}_{\ell}) \quad (127)$$

Now, we consider convexity in terms of the raw probability densities, $\mathbf{Q}(\mathbf{G}_1, \dots, \mathbf{G}_L)$. The ELBO can be written,

$$\mathcal{L} = \sum_{\ell=1}^L \mathbb{E}_{\mathbf{Q}(\mathbf{F}_1, \dots, \mathbf{F}_L)} \left[\sum_{\ell=1}^{L+1} \log \mathbf{P}(\mathbf{F}_{\ell} | \mathbf{F}_{\ell-1}) \right] + \mathbf{H}[\mathbf{Q}(\mathbf{F}_1, \dots, \mathbf{F}_L)]. \quad (128)$$

The expectation is linear in $\mathbf{Q}(\mathbf{F}_1, \dots, \mathbf{F}_L)$, and the entropy is concave in $\mathbf{Q}(\mathbf{F}_1, \dots, \mathbf{F}_L)$. So overall, the ELBO is concave in $\mathbf{Q}(\mathbf{F}_1, \dots, \mathbf{F}_L)$. Further, as $\mathbf{Q}(\mathbf{G}_1, \dots, \mathbf{G}_L)$ is linearly related to $\mathbf{Q}(\mathbf{F}_1, \dots, \mathbf{F}_L)$ (Eq. 127), the ELBO must also be concave in $\mathbf{Q}(\mathbf{G}_1, \dots, \mathbf{G}_L)$.

How does this relate to the work in the main text, where we optimize a single setting of $\mathbf{Q}(\mathbf{G}_1, \dots, \mathbf{G}_L)$? Our results for Langevin dynamics are exact, and if the true posterior over $\mathbf{G}_1, \dots, \mathbf{G}_L$ is a point (as we proved in the linear setting, and as our experiments suggest in the nonlinear setting), then Langevin sampling will converge to the true posterior. However, what if the true posterior actually has multiple modes (which does not seem to occur in our experiments, but which we have not been able to definitively rule out)? In that case, the deep kernel machine objective will have multiple modes, and Langevin sampling will converge to only one mode (note that Langevin sampling is not guaranteed to converge in our infinite dimensional setting (Roberts & Tweedie, 1996; Cheng & Bartlett, 2018), and therefore if multiple modes exist, it will converge to only one of them).

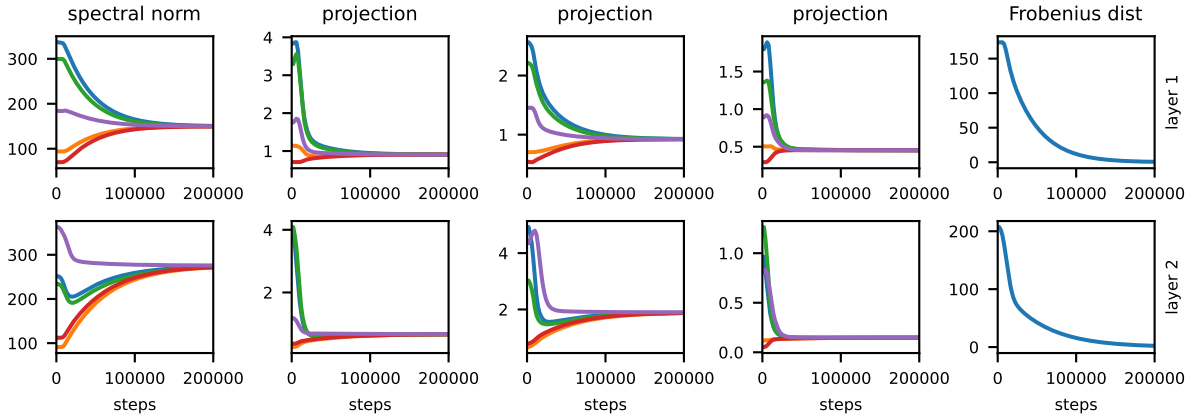


Figure 4: Two-layer deep kernel machine with squared exponential kernel trained on yacht.

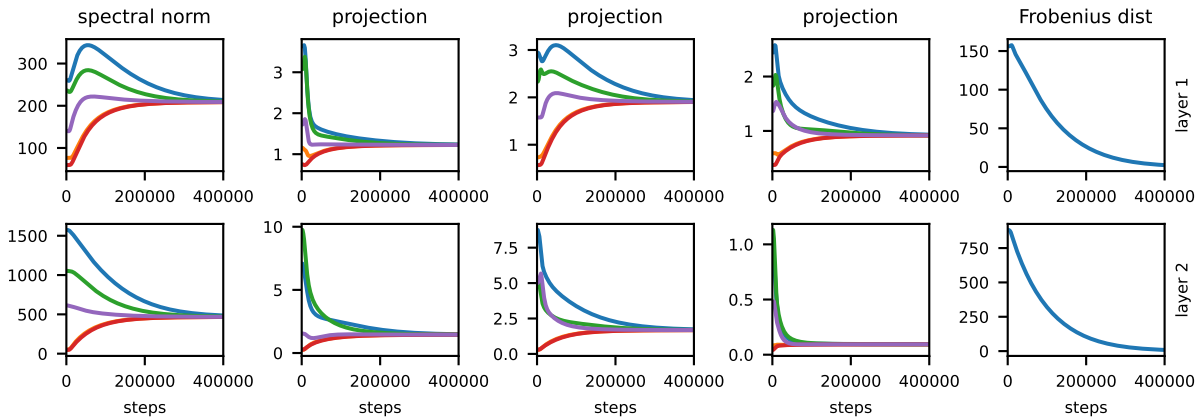


Figure 5: Two-layer deep kernel machine with ReLU kernel trained on yacht.

F Parameter settings

In our experiments, we first take the Cholesky decomposition $\mathbf{K}(\mathbf{G}_{\ell-1}) = \mathbf{L}_{\ell-1}\mathbf{L}_{\ell-1}^T$, then set $\mathbf{V}_\ell = \mathbf{L}_{\ell-1}\mathbf{\Xi}_\ell\mathbf{D}_\ell^{1/2}$ where each entry of $\mathbf{\Xi}_\ell \in \mathbb{R}^{P \times P}$ is independently sampled from a standard Gaussian, and \mathbf{D}_ℓ is a diagonal scaling matrix with each entry sampled i.i.d. from an inverse-Gamma distribution. The variance of the inverse-Gamma distribution is fixed to 100, and the mean is drawn from a uniform distribution $U[0.5, 3]$ for each seed. Since for any random variable $x \sim \text{Inv-Gamma}(\alpha, \beta)$, $\mathbb{E}(x) = \frac{\beta}{\alpha-1}$ and $\mathbb{V}(x) = \frac{\beta}{(\alpha-1)(\alpha-2)}$, once we fix the mean and variance we can compute α and β as

$$\alpha = \frac{\mathbb{E}(x)^2}{\mathbb{V}(x)} + 2, \quad (129)$$

$$\beta = \mathbb{E}(x)(\alpha - 1). \quad (130)$$

G Additional experiments

Here we present additional experiments for training two-layer DKMs with squared exponential or ReLU kernels on yacht (Fig. 4, Fig. 5), boston (Fig. 6, Fig. 7), energy (Fig. 8, Fig. 9) and concrete (Fig. 10, Fig. 11).

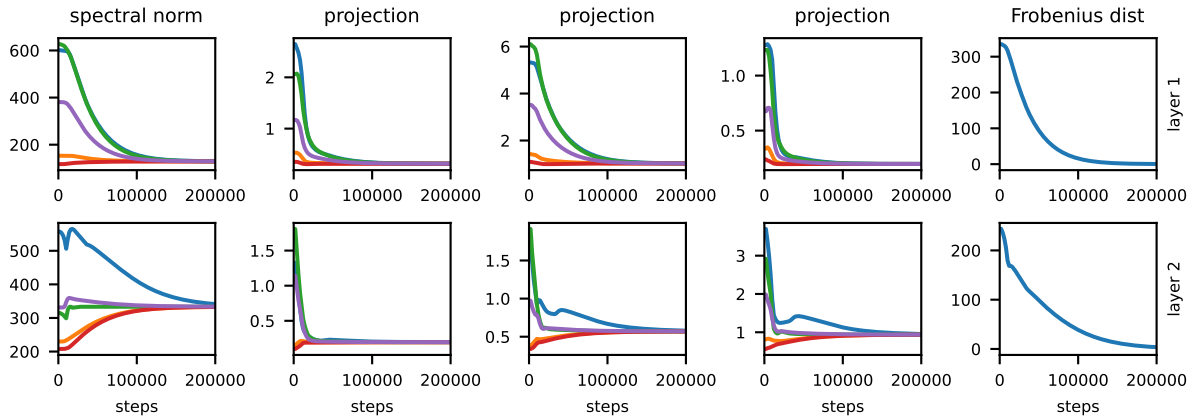


Figure 6: Two-layer deep kernel machine with squared exponential kernel trained on boston.

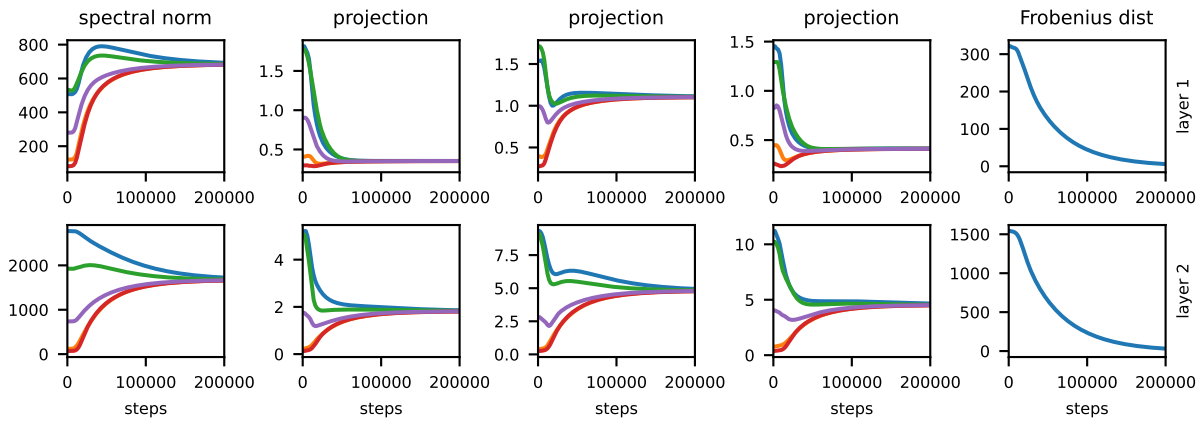


Figure 7: Two-layer deep kernel machine with ReLU kernel trained on boston.

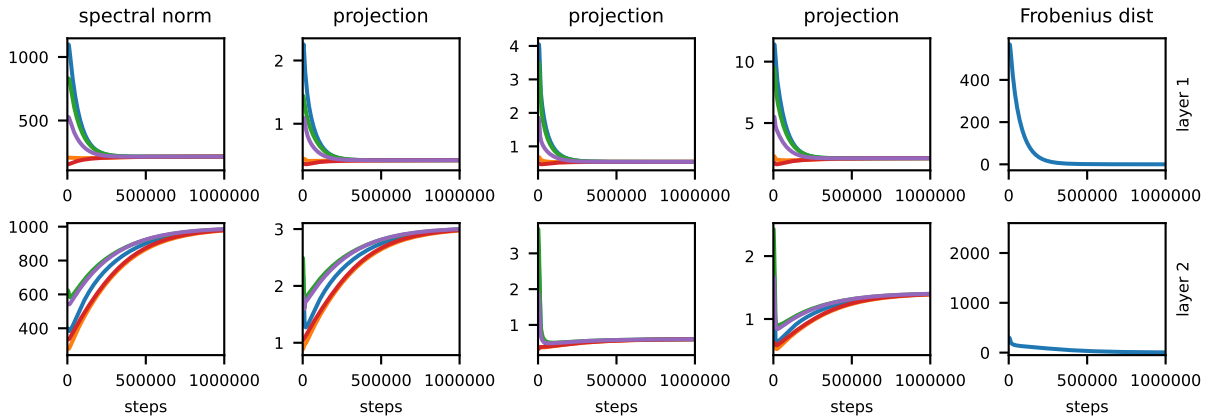


Figure 8: Two-layer deep kernel machine with squared exponential kernel trained on energy.

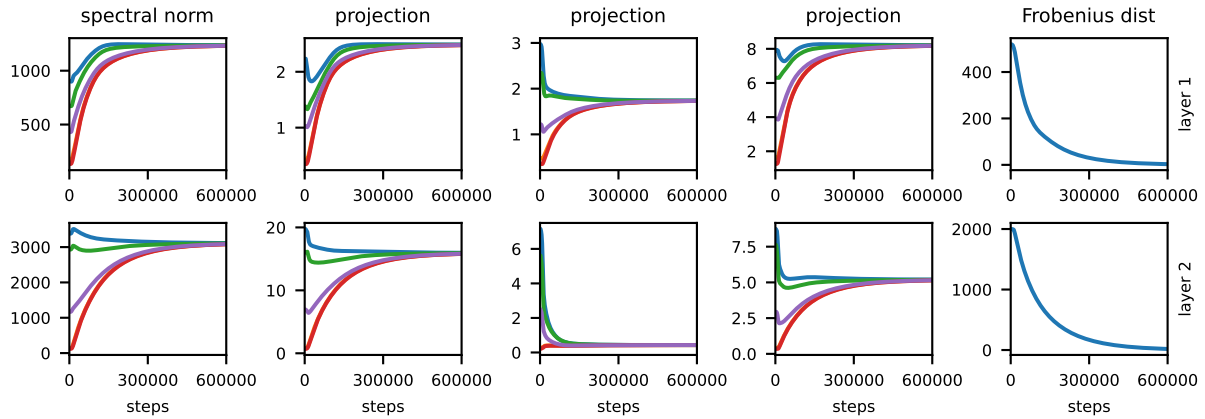


Figure 9: Two-layer deep kernel machine with ReLU kernel trained on energy.

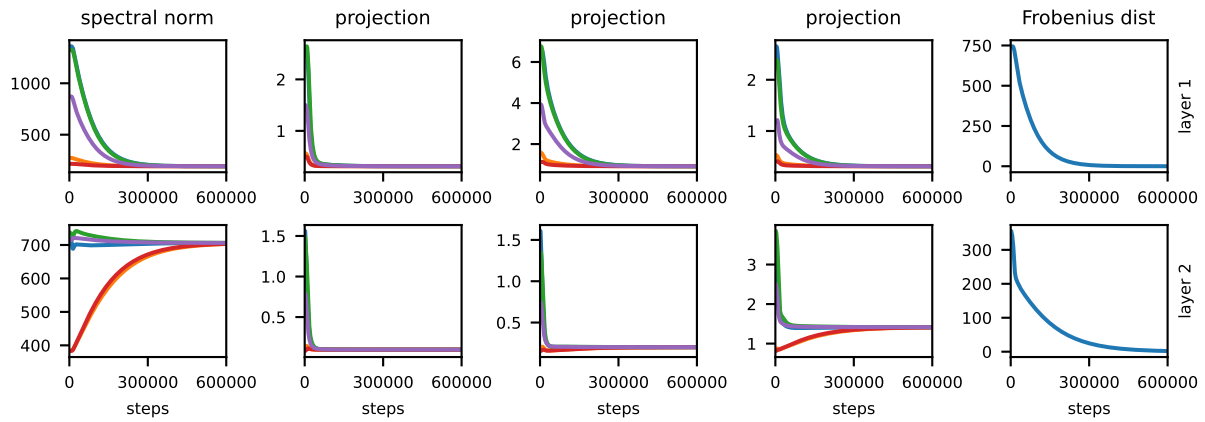


Figure 10: Two-layer deep kernel machine with squared exponential kernel trained on concrete.

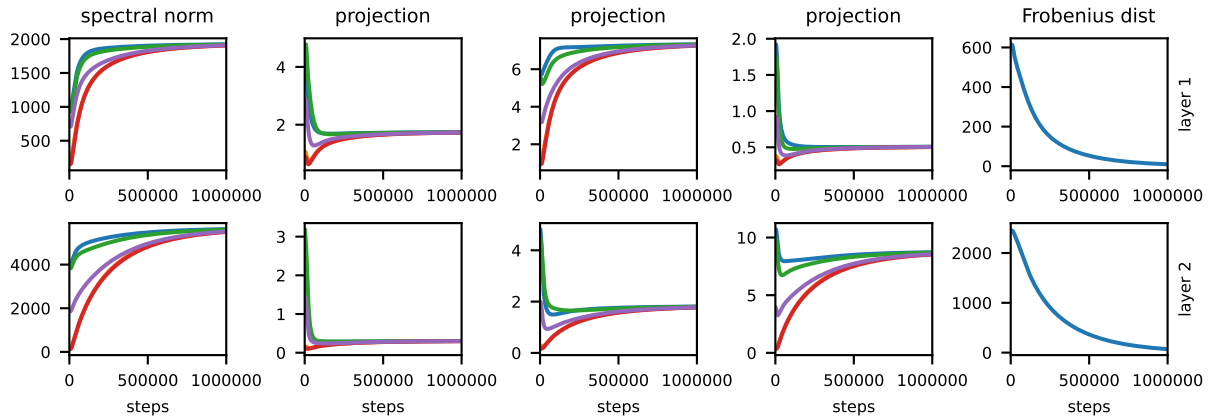


Figure 11: Two-layer deep kernel machine with ReLU kernel trained on concrete.